DE GRUYTER
OPEN

Acta Palaeobotanica 58(2): 135–157, 2018
DOI: 10.2478/acpa-2018-0016

e-ISSN 2082-0259
ISSN 0001-6594

# Exceptionally well-preserved Early Cretaceous leaves of *Nilssoniopteris* from central Mongolia

FABIANY HERRERA[1,5,*], GONGLE SHI[2], GOMBOSUREN TSOLMON[3], NIIDEN ICHINNOROV[3], MASAMICHI TAKAHASHI[4], PETER R. CRANE[5,6] and PATRICK S. HERENDEEN[1]

[1]Chicago Botanic Garden, Glencoe, Illinois 60022 USA; e-mails: fherrera@chicagobotanic.org; pherendeen@chicagobotanic.org

[2]State Key Laboratory of Palaeobiology and Stratigraphy, Nanjing Institute of Geology and Palaeontology and Center for Excellence in Life and Paleoenvironment, Chinese Academy of Sciences, Nanjing 210008 People's Republic of China; e-mail: glshi@nigpas.ac.cn

[3]Institute of Paleontology and Geology, Mongolian Academy of Sciences, Ulaanbaatar-51, Mongolia; e-mails: tsolmonpaleo205@gmail.com; iichka@yahoo.com

[4]Department of Environmental Sciences, Niigata University, Ikarashi, Nishi-ku, Niigata 950-2181 Japan; e-mail: masamichi@env.sc.niigata-u.ac.jp

[5]Oak Spring Garden Foundation, Upperville, Virginia 20184 USA

[6]School of Forestry and Environmental Studies, Yale University, New Haven, Connecticut 06511 USA; e-mail: peter.crane@yale.edu

Received 20 June 2018; accepted for publication 25 October 2018

ABSTRACT. Two new Early Cretaceous (Aptian-Albian) species of fossil bennettitalean leaves are described from central Mongolia and assigned to the genus *Nilssoniopteris*. *Nilssoniopteris tomentosa* F.Herrera, G.Shi, Tsolmon, Ichinnorov, Takahashi, P.R.Crane, et Herend. sp. nov., isolated from bulk sediment samples collected for mesofossils in the Tevshiingovi Formation at the Tevshiin Govi opencast coal mine, is distinctive in having a dense, well-developed indumentum composed of branched, flattened multicellular trichomes on the abaxial leaf surface. This species provides the first direct evidence of complex multicellular trichomes in Bennettitales and adds to the evidence of leaf anatomical features in the group that were probably advantageous in increasing water use efficiency and/or perhaps had other functions such as deterring insect herbivory. Comparison with other well-preserved leaves of Bennettitales, including *Nilssoniopteris shiveeovoensis* F.Herrera, G.Shi, Tsolmon, Ichinnorov, Takahashi, P.R.Crane, et Herend. sp. nov., collected as hand specimens from the Khukhteeg Formation at the Shivee Ovoo locality, suggests that the trichome bases seen commonly on the abaxial cuticle of bennettitalean leaves bore trichomes with very low fossilization potential. In some cases these trichomes may have been shed as the leaves matured, but in other cases they probably decayed during diagenesis or were destroyed during the standard processes by which fossil leaf cuticles are prepared.

KEYWORDS: insect herbivory, mesofossils, mesophytic, *Nilssoniopteris*, paleoecology, trichomes, xerophytic

## INTRODUCTION

Leaves of Bennettitales are among the more common fossils in Jurassic and Early Cretaceous fossil floras. A few bennettitalean leaves have been described from permineralized material (e.g. Yamada et al. 2009, Ray et al. 2014) but most of the better-known species are based on compression fossils that have yielded well-preserved cuticles (e.g. Harris 1969, Watson & Sincock 1992, Boyd 2000, Cleal & Rees 2003, Pott et al. 2007). Most bennettitalean leaves consist of an elongated main rachis either with more or less distinct pinnae (e.g. *Otozamites*) or with a segmented, pinnately arranged lamina (e.g. *Anomozamites*). However, in *Nilssoniopteris* the leaves are simple and the leaf lamina is almost entire, which is

* Corresponding author

unusual in the Bennettitales as a whole. The plants that bore *Nilssoniopteris* are also of interest because two species of *Nilssoniopteris* have been associated with the bisexual bennettitalean flowers assigned to *Williamsoniella* (Thomas 1916, Thomas & Batten 2001, Crane & Herendeen 2009).

An interesting feature of the leaves of Bennettitales is that even in otherwise apparently mesomorphic vegetation, for example the Middle Jurassic flora of Yorkshire, the leaves of Bennettitales exhibit seemingly xeromorphic features, including reflexed pinnae, well-developed papillae on the abaxial surface, sunken stomata, and stomatal pits that are occluded to various degrees and often overarched by epidermal papillae (e.g. Harris 1969). In addition, bennettitalean leaves from the Early Cretaceous Wealden flora show circular, subsurface, multicellular bodies resembling the salt glands of extant plants, which remove excess salts absorbed from saline or arid soils (Sincock & Watson 1988, Watson & Alvin 1996).

In this paper we provide further evidence of anatomical features that are likely linked to increased water use efficiency in Bennettitales, through description of a new Early Cretaceous species of *Nilssoniopteris* based on exceptionally well-preserved material from Mongolia. This species is distinctive in having a dense, very well developed and exquisitely preserved indumentum on the abaxial leaf surface. Careful examination of the indumentum provides the first direct evidence of complex multicellular trichomes in Bennettitales. Comparison with other well-preserved leaves of Bennettitales, including an additional new species from another Early Cretaceous locality in Mongolia, suggests why the trichome bases seen commonly on the abaxial cuticle of bennettitalean leaves rarely have the trichomes themselves preserved.

## MATERIALS AND METHODS

The fossils described in this study come from two Early Cretaceous opencast coal mines in central Mongolia: Tevshiin Govi (45°58′54″N, 106°07′12″E), ca 220 km SW of Ulaanbaatar; and Shivee Ovoo (46°13′47.4″N, 108°54′8″E), ca 40 km SE of Choyr.

The fossil leaves and bract scales from Tevshiin Govi were recovered as mesofossils from unconsolidated sediments of the Tevshiingovi Formation, a sequence of conglomerates, sandstones and siltstones with thick coal and lignite seams. The Tevshiingovi Formation is considered to be Aptian-Albian in age (125–99.6 Mya) based on stratigraphic correlations (Graham et al. 2001, Erdenetsogt et al. 2009, Hasegawa et al. 2018) and on palynomorphs recovered from the plant localities (Ichinnorov 2003, Nichols et al. 2006, Ichinnorov et al. 2012). The mesofossils described here were recovered from only three (PSH177, PSH286, PSH287) of the more than 49 bulk sediment samples from the Tevshiin Govi mine. All three samples were from a channel deposit of medium-grained sandstone containing abundant lenses rich in organic matter. This sandstone lies on top of a thick lignite deposit which has been much more extensively sampled and contains abundant exceptionally well-preserved conifers, ferns and other seed plants (Leslie et al. 2013, Shi et al. 2014, 2016, 2018, Herrera et al. 2015, 2016, 2017a,b,c). The Tevshiin Govi bulk samples were disaggregated in water and hydrogen peroxide. Mesofossils were then cleaned with hydrochloric and hydrofluoric acids using standard techniques (Penny 1999, Wellman & Axe 1999).

The fossil leaves from the Shivee Ovoo locality were collected as compression macrofossils from blocks of weakly consolidated fine-grained sandstones/siltstones of the Khukhteeg Formation (equivalent to the Tevshiingovi Formation). The Khukhteeg Formation is composed of a complex sequence of conglomerates, sandstones, siltstones and coal seams. The Khukhteeg Formation is also considered to be Aptian-Albian in age (125–99.6 Mya; Ichinnorov 1996, Hasegawa et al. 2018).

Leaf cuticles from mesofossils and compression fossils were prepared using standard techniques (Kerp & Krings 1999). The cuticles were macerated in dilute household bleach (ca 1% sodium hypochlorite solution) for several seconds to several minutes depending on the preservation of the fossils, and monitored carefully to ensure optimal preparations. Isolated cuticles were mounted on slides with glycerine jelly, which were then sealed using nail polish. Fossils were photographed (LM) using a Canon Rebel camera with 100 mm macrolens attached to a Stackshot system, and digital images were merged using Helicon Focus software. Cuticles were examined and photographed with differential interference contrast (DIC) illumination using a Leica DMLB microscope at the Chicago Botanic Garden, and with an Olympus BX53 microscope at the Nanjing Institute of Geology and Palaeontology, CAS. Scanning electron microscopy (SEM) was done using a Carl Zeiss EVO 60 scanning electron microscope at the Field Museum, Chicago, and a Leo1530 VP field-emission scanning electron microscope at the Nanjing Institute of Geology and Palaeontology, CAS, Nanjing, China.

Leaves and bracts of Bennettitales from several Early Cretaceous localities in Mongolia that were described by Krassilov (1982) were reexamined from the collections of the Institute of Biology and Soil Science, Far East Branch, Russian Academy of Sciences in Vladivostok, Russia. Fossil material described in this study is housed in the palaeobotanical collections of the Field Museum, Chicago (FMNH: collection numbers with the prefix PP), and in the Institute of Paleontology and Geology in Ulaanbaatar, Mongolia (Mongolian Paleontological Center-Flora; with the prefix MPCFL).

## SYSTEMATICS

### Order: BENNETTITALES Wieland

### Genus: *Nilssoniopteris* Nathorst emend. Zhao et al. 2018

### Species: ***Nilssoniopteris tomentosa*** F.Herrera, G.Shi, Tsolmon, Ichinnorov, Takahashi, P.R.Crane, et Herend. sp. nov.

Specific diagnosis. Leaf petiolate. Lamina strap-shaped, ca 12.5–28 mm long, undivided, and attached to adaxial surface of midrib. Lamina margin entire. Numerous lateral, parallel veins entering lamina at ca 70–90° and ending at leaf margin. Lateral vein density 30–40 veins per cm in middle region of leaf, and 60–80 veins per cm in proximal and distal regions. Lateral veins unbranched or commonly dichotomizing close to midrib and also exmedially. Leaf lamina hypostomatic; adaxial and abaxial cuticles thick. Midrib lacking stomata but covered with trichomes. Cuticle with brachyparacytic (syndetocheilic) stomatal complexes arranged in poorly defined irregular bands, each composed of 2–4 files of stomatal complexes. Stomatal complexes oriented with their long axes perpendicular to lateral veins or sometimes slightly oblique. Each stomatal complex consisting of a pair of guard cells flanked by two subsidiary cells. Each subsidiary cell bearing a single, large, solid papilla overarching the stomatal aperture. Stomatal density ca 65–82 complexes per square mm. Trichomes and trichome bases extremely dense on abaxial side of leaf lamina only. Trichome bases mainly two-celled, occasionally one-celled. Trichomes flattened, multicellular and branched; branches ending in tapered and spine-like tip. Trichomes forming dense tomentose covering on adaxial surface of lamina, midrib and petiole.

Holotype. PP56982; Pl. 1, fig. 1.

Other material. PP56983–PP56993, PP56998–PP57005, PP57007–57010; Pl. 1, figs 2–6, Pl. 2, Pl. 3, Pl. 4, Pl. 10 figs 1–5.

Repository. Paleobotanical Collections, Department of Geology, The Field Museum, Chicago, Illinois, USA.

Stratigraphic position and age. Tevshiingovi Formation, Aptian–Albian stage (125–99.6 Mya), Early Cretaceous.

Locality. Tevshiin Govi coal mine (45°58′54″N, 106°07′12″E), central Mongolia; sample nos. PSH177, PSH286, PSH287.

Etymology. From Latin *tomentum*, widely used in botany to mean “covered with a dense layer of short hairs”.

Detailed description. The specimens described here occur in only three samples from the Tevshiin Govi deposit. The specimens are abundant but all are incomplete.

Leaves petiolate (Pl. 1, fig. 4); petiole at least 20.1 mm long and 4.3 mm wide (measured at widest point). Midrib stout, transversely striated, and ca 2–4.3 mm wide (measured near base; Pl. 1, fig. 2). Leaf lamina at least ca 12.5–28 mm long and 8–15 mm wide. Lamina strap-shaped, undivided (not subdivided into segments) and attached to adaxial surface of midrib, leaving part of upper surface of midrib exposed (Pl. 1, figs 1–4). Lamina margin entire. Apex slightly acuminate and asymmetrical, with midrib ending at tip (Pl. 1, fig. 2). Base asymmetrical, convex to slightly cordate (Pl. 1, figs 1, 2, 4). Numerous lateral, parallel veins entering lamina, with density of 30–40 veins per cm in middle region of leaf to 60–80 veins per cm in proximal and distal regions. Lateral veins commonly dichotomizing close to midrib but also exmedially, also free and unbranched (Pl. 1, figs 1, 2, 4–6); all lateral veins slightly curving exmedially just before ending at margin (Pl. 1, fig. 5). Lateral veins inserted on midrib at ca 85–90° proximally to 68–75° medially and distally. Lateral veins equal in thickness and frequently visible on both sides of lamina, although in many specimens visible only on adaxial leaf surface (Pl. 1, figs 1, 2).

Midrib epidermal cells isodiametric, mostly square, regularly rectangular to elongate in outline, arranged in longitudinal files on both adaxial and abaxial cuticle (Pl. 2, fig. 1, Pl. 3, fig. 1). Square to nearly square cells ranging from 12 to 43 μm; rectangular to more longitudinally elongated cells ranging from 12 to 22 μm wide and from to 27 to 64 μm long. Midrib lacking stomata, but trichome bases (ca 23–50 μm diam.) present on abaxial leaf surface (Pl. 2, fig. 1, Pl. 3, fig. 1). Periclinal walls smooth and slightly punctate. Anticlinal walls smooth, straight to moderately sinuous.

Leaf lamina hypostomatic. Cuticles of both adaxial and abaxial leaf surfaces thick and well

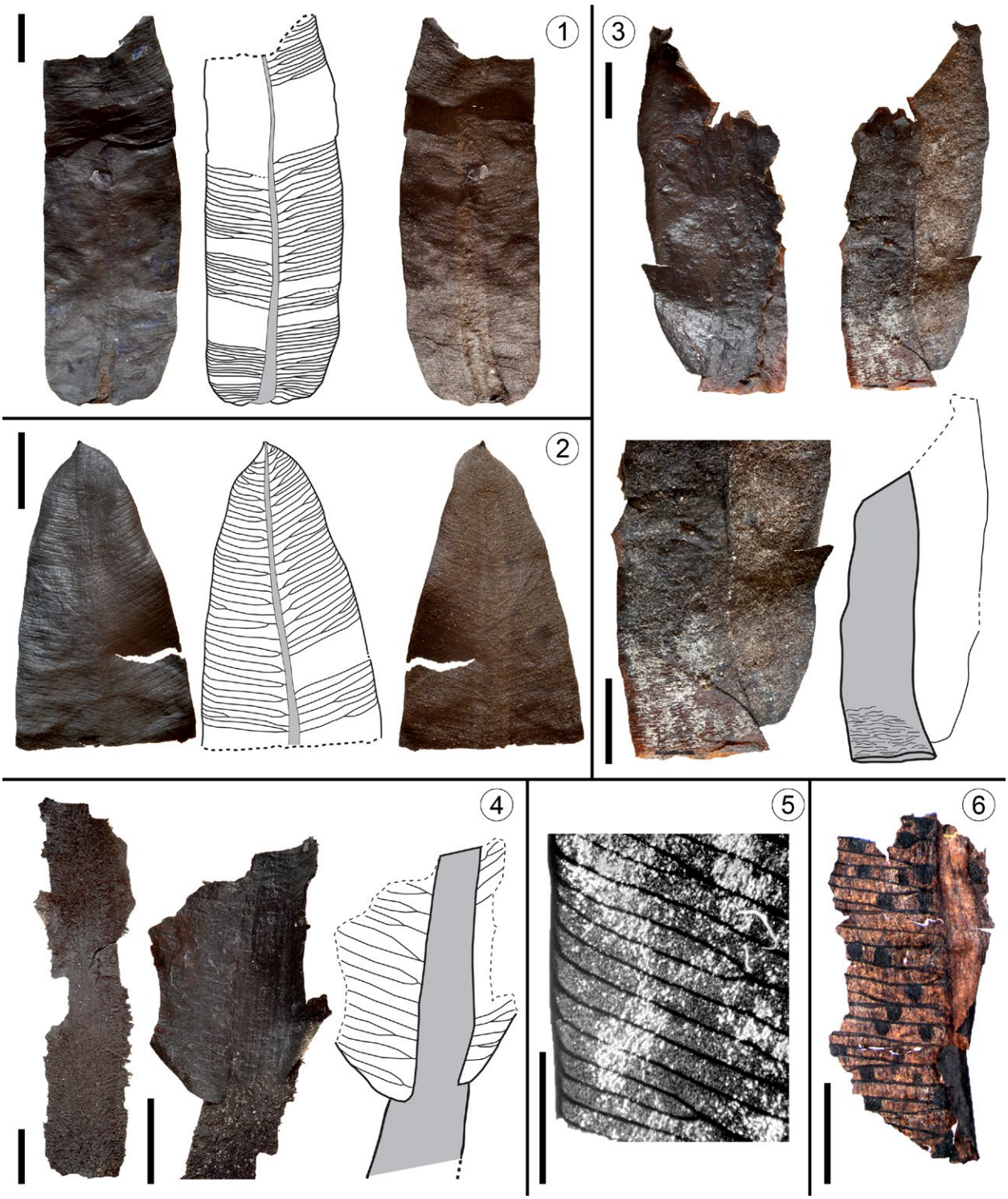


**Plate 1**. Early Cretaceous leaves of *Nilssoniopteris tomentosa* sp. nov. from Tevshiin Govi. Light micrographs and line drawings. **1**. Holotype (PP56982), showing leaf base and midrib; leaf apex missing. Left, adaxial surface; center, line drawing of adaxial surface, showing stout midrib and dichotomizing lateral veins; right, abaxial surface, showing light brown/red-brownish color; **2**. Leaf fragment, showing acute, slightly acuminate apex. Left, adaxial surface; center, line drawing of adaxial surface, showing stout midrib and dichotomizing lateral veins; right, abaxial surface, showing light brown/red-brownish color (PP56983); **3**. Leaf fragment, showing basal part of lamina. Upper left, adaxial surface; upper right, abaxial surface, showing stout midrib with transverse striations; bottom left, detail of leaf base, showing broad, stout midrib; bottom right, line drawing from figure on upper right, showing stout midrib in grey (PP56984); **4**. Leaf fragment, showing basal part of leaf lamina, midrib and petiole. Left, abaxial surface, showing petiole and midrib covered with tomentose trichomes; center, detail of leaf base from adaxial surface; right, line drawing of leaf base from adaxial surface, showing stout midrib/petiole (dark grey) and insertion of lamina into upper part of midrib (PP56985); **5**. Portion of cleared leaf from near leaf margin, showing dichotomous and unbranched lateral veins that curve exmedially toward leaf apex (PP56986); **6.** Fragment of adaxial leaf cuticle, showing leaf lamina with several lateral veins dichotomizing close to midrib. Dark spots represent wound tissue likely caused by insect galls (PP56987). All scale bars = 3 mm

preserved. Adaxial leaf surface lacking stomata, consisting almost entirely of epidermal cell outlines that are isodiametric (Pl. 3, fig. 2), usually rectangular to square, ca 20–46 µm long and ca 15–35 µm wide. Periclinal walls smooth to finely granular. Outer surface of adaxial cuticle lacking papillae, trichomes or hair bases. Anticlinal walls well cutinized with uneven thickenings, and strongly sinuous with tightly spaced folds (Ω-shaped; Pl. 3, fig. 2). Abaxial cuticle consisting of epidermal cells, usually rectangular to square in outline, ca 18–50 µm long and ca 13–40 µm wide (Pl. 2, fig. 2). Periclinal walls smooth to finely granular. Anticlinal walls well cutinized, with uneven thickenings, strongly sinuous with tightly spaced folds (Ω-shaped; Pl. 3, fig. 5). Abaxial epidermis with trichomes and hair bases on outer cuticular surface (see description below).

Abaxial cuticle with brachyparacytic (syndetocheilic) stomatal complexes arranged in poorly defined irregular bands composed of 2–4 files, ca 145–320 µm wide (Pl. 2, figs 2–6, Pl. 3, figs 3–8). Stomatal bands oriented parallel to lateral veins, one band between two lateral veins (Pl. 2, fig. 2, Fig. 1A). Stomatal complexes frequently oriented with their long axes perpendicular to the lateral veins, or in some cases slightly oblique at ca 10–41°. Stomatal density ca 65–82 complexes per square mm. Stomatal complexes usually appearing crowded but never directly sharing lateral subsidiary cells; stomatal complexes also occurring ± isolated within stomatal band and separated by one or two normal epidermal cells (Pl. 2, figs 3–6, Pl. 3, figs 5–8).

Stomatal complexes ca 25–38 µm long (distance between polar walls of guard cells) and 21–45 µm wide (distance between outermost walls of lateral subsidiary cells), and ± elliptical in outline. Stomatal complexes sunken, each consisting of a pair of guard cells with two subsidiary cells (Pl. 2, figs 3–6, Pl. 3, figs 3–8). Outer surface of cuticle over guard cells and subsidiary cells ± smooth (Pl. 3, figs 3, 4). Each subsidiary cell bearing a single, large, solid papilla overarching the stomatal aperture (Pl. 2, fig. 6, Pl. 3, fig. 3); subsidiary cell papillae occasionally appearing poorly developed, but stomatal aperture appearing occluded by thickened subsidiary cells (Pl. 3, fig. 4). Stomatal aperture slit-like to rarely pore-like, oriented parallel to lateral subsidiary cells and flanked by two heavily cutinized lips (8.2–9.1 µm long, 1.2–2.0 µm wide). Cuticular flanges between guard cells and subsidiary cells strongly developed and butterfly-shaped (Pl. 3, figs 5–8). Guard cells 21–29 µm long, 10–14 µm wide, regularly crescent-shaped in outline, strongly sunken, and with strongly cutinized dorsal thickenings and polar extensions (Pl. 2, figs 3–6, Pl. 3, figs 5–8). Guard cells commonly of unequal lengths in the same stomatal complex and flanked by two lateral subsidiary cells. Subsidiary cells visible, 23–37 µm long, 14–20 µm wide, with flange of outer wall irregular serrate or sinuous to convex, symmetrical or asymmetrical in outline, oriented parallel to stomatal aperture and extending beyond length of guard cells (Pl. 2, figs 5–6, Pl. 3, figs 6–8).

Three-dimensionally preserved trichomes and trichome bases extremely dense on abaxial leaf surface only, including on midrib, stomatal bands and veins (Pl. 4). On petiole, trichomes occur on both abaxial and adaxial surfaces (Pl. 1, fig. 4). Well-preserved and densely spaced three-dimensional trichomes result in a difference in color between abaxial and adaxial leaf surfaces, which are light brown/red brown and dark brown/black respectively (Pl. 1, figs 1–3). Individual trichomes ca 400–800 µm long and 70–120 µm wide, multicellular, distinctly flattened, and branched (i.e. trichomes treelike and dendritic, with central main axis and multiple lateral branches) (Pl. 4, figs 3–6). Up to 15–20 lateral branches present on each trichome. Each lateral branch ending in tapered spine-like tip (ca 70–180 µm long).

On inner surface of abaxial leaf cuticle, trichome bases measure 20–55 µm in diameter. Trichome bases elliptical in outline, generally consisting of two cells and with sinuous and tightly folded, thickened margin (Pl. 10, figs 1–3). Trichome bases sometimes one-celled, rarely three- or four-celled. Trichome density ca 72–95 bases per square mm. Trichome bases on outer surface of leaf cuticles appearing as broken remains or thickened rings (14–23 µm in diameter; Pl. 10, figs 4, 5).

### Associated *Cycadolepis* sp. bract-scales

Two *Cycadolepis* bract-scales were recovered in samples PSH286 and PSH287 from Tevshiin Govi (Pl. 5, Pl. 6). They are 6.6–9.5 mm long, 7.5–9.3 mm wide, 100–200 µm thick, broadly ovate in outline, with conspicuous acuminate apex. Tapered apex of scale ca 1.9–4.5 mm

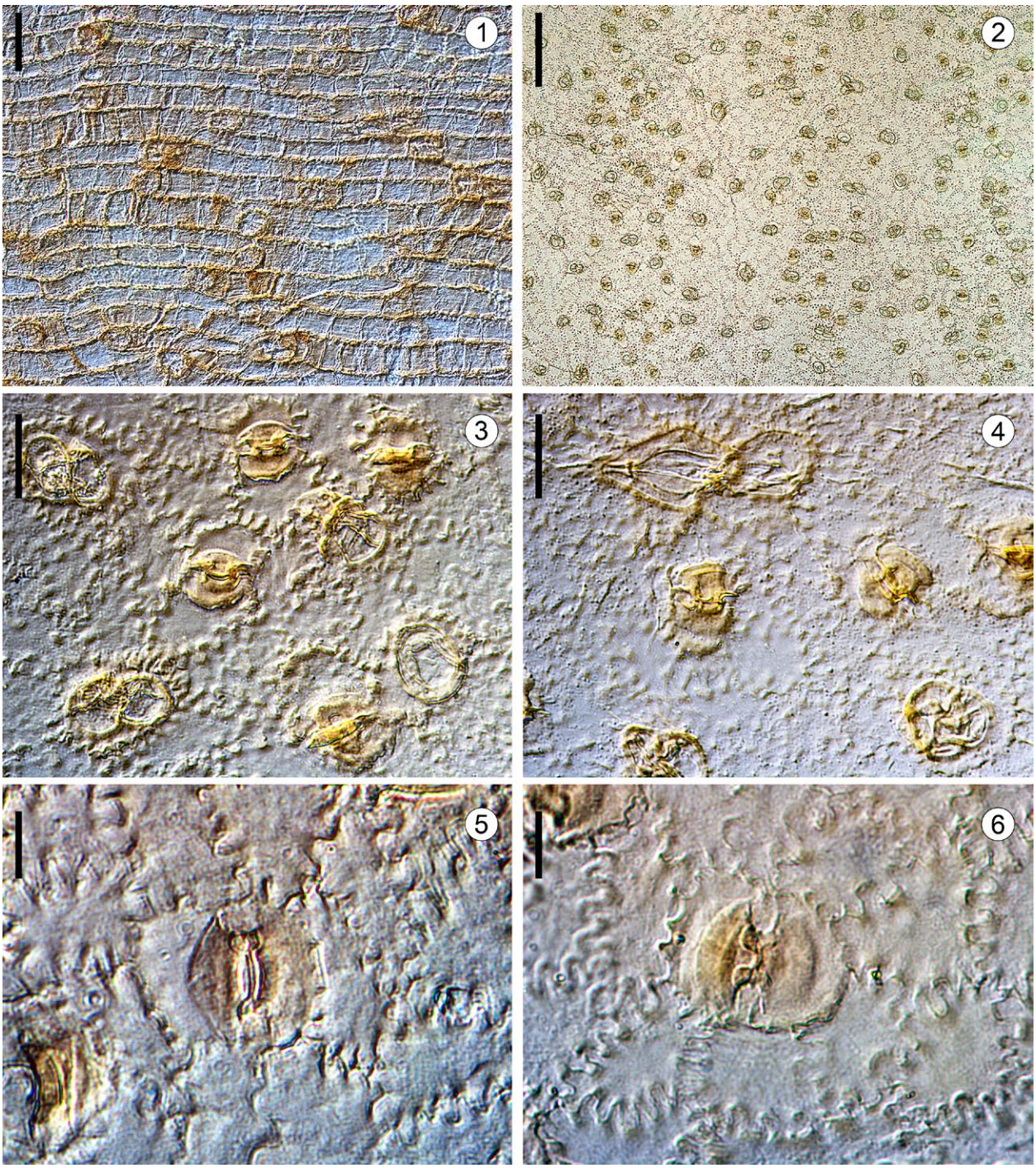


**Plate 2**. Early Cretaceous leaves of *Nilssoniopteris tomentosa* sp. nov. from Tevshiin Govi. Light micrographs of leaf cuticles and stomata. **1**. Abaxial cuticle of midrib (oriented horizontally), showing elongate rectangular to square epidermal cell outlines arranged in longitudinal files; note abundant trichome bases (PP56988); **2**. Abaxial cuticle of leaf lamina (oriented vertically), showing arrangement of stomata and trichome bases; note at least three very poorly defined stomatal bands (see Fig. 1) (PP56989); **3**. Abaxial cuticle of leaf lamina, showing epidermal cell outlines with sinuous anticlinal walls, four stomata with prominently cutinized thickenings of guard cells, and four trichome bases (PP56989); **4**. Abaxial cuticle, showing epidermal cell outlines with sinuous anticlinal walls, three stomata with prominently cutinized thickenings of guard cells, and three trichome bases (PP56989); **5**. Detail of abaxial cuticle, showing strongly sinuous epidermal cell outlines and a brachyparacytic (syndetocheilic) stomatal complex with prominently cutinized thickenings of guard cells. (PP56989); **6**. Detail of abaxial cuticle, showing strongly sinuous epidermal cell outlines and a brachyparacytic (syndetocheilic) stomatal complex; micrograph focused on subsidiary cell papillae (PP56989). Scale bars = 200 μm (2); 50 μm (3, 4); 40 μm (1); 20 μm (5, 6)

long, ending in spine-like or rounded tip. Scale margin entire. Scales coriaceous, often with transverse wrinkles, and thick cuticle (Pl. 5, figs 1, 2).

Cuticle from adaxial and abaxial surfaces of the scales showing rectangular to polygonal epidermal cell outlines arranged in ± regular longitudinal files, 10–42 μm long, 14–35 μm

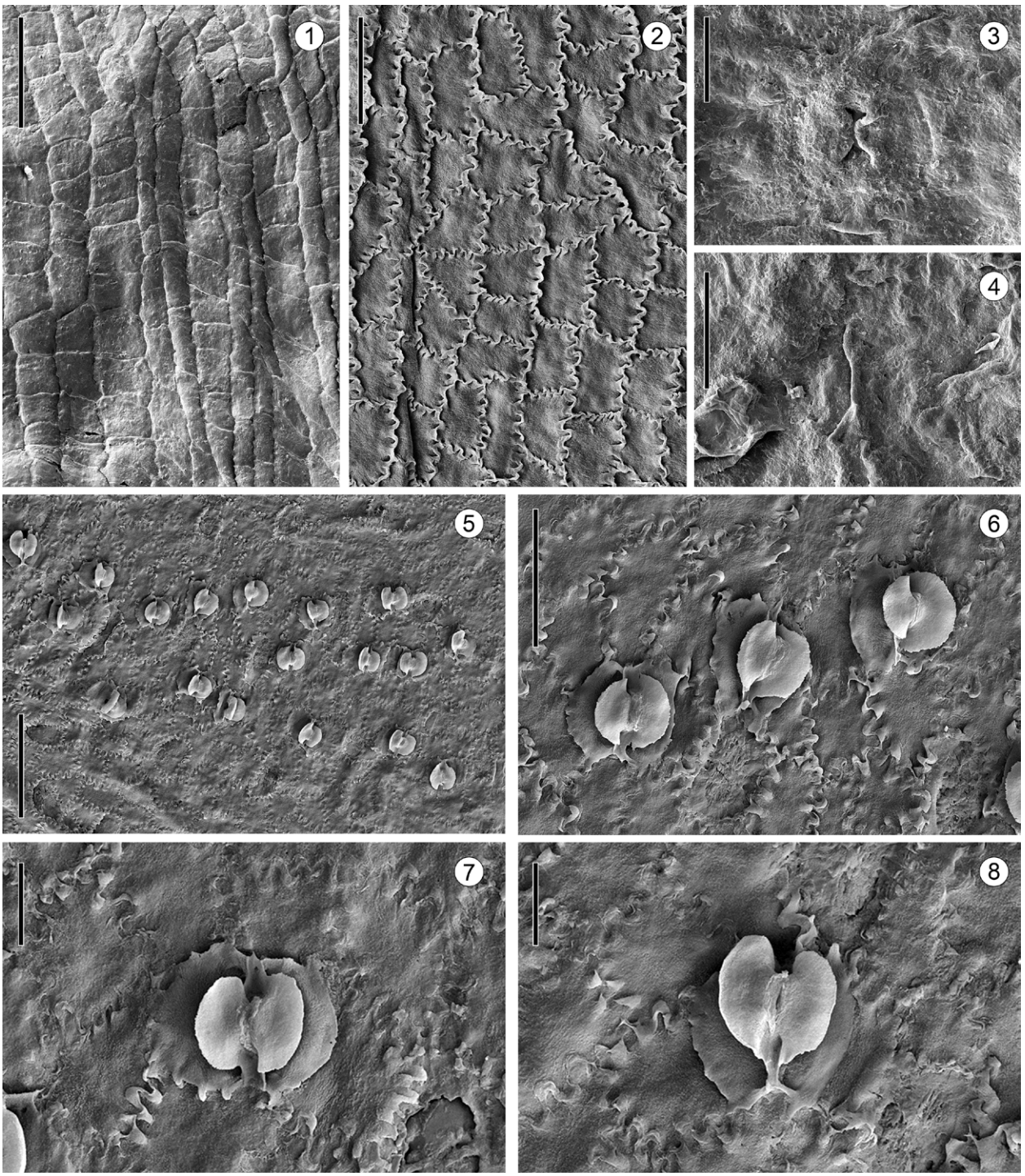


**Plate 3**. Early Cretaceous leaves of *Nilssoniopteris tomentosa* sp. nov. from Tevshiin Govi. SEM micrographs of leaf cuticles and stomata. **1**. Inner surface of abaxial cuticle of midrib, showing elongate rectangular to square epidermal cell outlines arranged in longitudinal files (PP56990); **2**. Inner surface of adaxial cuticle, showing epidermal cell outlines demarcated by cutinized, strongly sinuous and tightly spaced folds of anticlinal flanges (PP57009); **3**. Outer surface of abaxial cuticle, showing stomatal pit and subsidiary cells bearing large, solid papillae overarching the stomatal aperture. (PP57007); **4**. Outer surface of abaxial cuticle, showing strongly occluded stomatal aperture and thickened subsidiary cells; note trichome base at bottom left (PP57007); **5**. Inner surface of abaxial cuticle (oriented horizontally), showing 18 stomata in poorly defined stomatal band (PP56991); **6**. Detail from Plate 3, Fig. 4, showing three brachyparacytic (syndetocheilic) stomatal complexes; **7**. Detail from Plate 3, Fig. 4, showing stoma with pair of guard cells with two subsidiary cells; **8**. Detail from Plate 3, Fig. 4, showing stoma with pair of guard cells with two subsidiary cells. Scale bars = 100 μm (1, 5); 50 μm (2, 6); 20 μm (3, 4, 7, 8)

wide (Pl. 6, figs 1, 2). Anticlinal walls of epidermal cells straight or slightly curved, with thick, well-developed cuticular flanges. Periclinal walls ± smooth, lacking cuticular thickenings or papillae. Stomata very rare on adaxial and abaxial surfaces of scales, randomly distributed and oriented (Pl. 6, fig. 2). Stomatal complexes ca 18–22 μm long and 18–20 μm wide, ± elliptical

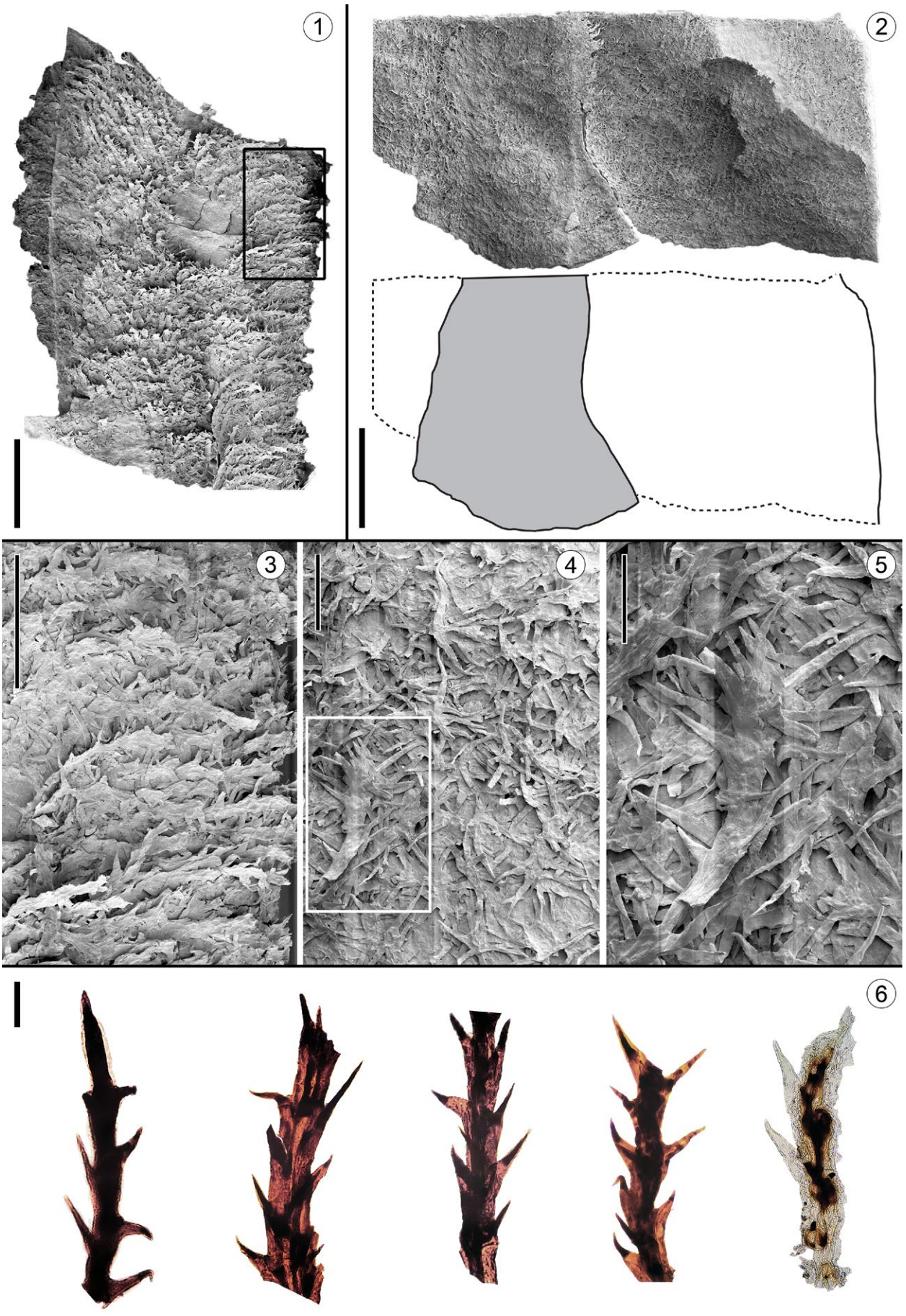
1
2
3
4
5
6

in outline, consisting of a pair of sunken guard cells flanked by two subsidiary cells.

Three-dimensionally preserved trichomes present on both surfaces of scale but abundant only on presumed adaxial surface (Pl. 5, figs 1, 2, left). On presumed abaxial surface, trichomes occur only on acuminate apex and along scale margin (Pl. 5, figs 1, 2, right). Trichomes forming tightly imbricate, tomentose covering (Pl. 6, figs 3–5). Trichomes at least ca 400–1300 μm long and 40–70 μm wide, multicellular, flattened, with bases commonly circular, and branched (i.e. dendritic trichomes with central main axis and multiple lateral branches; Pl. 6, figs 3–6). Up to 15–20 branches present on each trichome, with each lateral branch ending in tapered and spine-like tip (34–125 μm long).

Material. PP56994–PP56996; Pl. 5, Pl. 6.

Repository. Paleobotanical Collections, Department of Geology, The Field Museum, Chicago, Illinois, USA.

Stratigraphic position and age. Tevshiingovi Formation, Aptian–Albian stage (125–99.6 Mya), Early Cretaceous.

Localities. Tevshiin Govi coal mine (45°58′54″N, 106°07′12″E), central Mongolia; sample nos. PSH286, PSH287.

### Comments on *Nilssoniopteris tomentosa* and *Cycadolepis* sp.

Leaves of *Nilssoniopteris tomentosa* and the *Cycadolepis* bract-scales have not been found in organic connection but they were likely produced by the same plant species. They are the only bennettitalean fossils recovered at the Tevshiin Govi locality, and the *Cycadolepis* bracts occur in two of the three samples that contain *N. tomentosa* (PSH286 and PSH287). Both the leaves and the bracts have thick cuticles with similar brachyparacytic (syndetocheilic) stomatal complexes. Most significantly, both the leaves and bract-scales preserve the same multicellular, flattened and branched trichomes (Pl. 4, Pl. 6).

### Species: ***Nilssoniopteris shiveeovoensis*** F.Herrera, G.Shi, Tsolmon, Ichinnorov, Takahashi, P.R.Crane, et Herend. sp. nov.

Specific diagnosis. Leaf petiolate. Lamina strap-shaped, long and narrow (15–19 cm long), undivided, and attached to adaxial surface of midrib. Lamina margin entire. Numerous lateral, parallel veins entering lamina at ca 45–90° and ending at leaf margin. Lateral vein density ca 25–40 veins per cm in middle region of leaf, and ca 30–50 veins per cm in proximal and distal regions. Lateral veins unbranched or more commonly dichotomizing, either close to midrib or exmedially. Midrib with trichome bases but few stomata. Leaf lamina hypostomatic; adaxial and abaxial cuticle thick. Cuticle with brachyparacytic (syndetocheilic) stomatal complexes arranged in poorly defined irregular bands, each composed of 1–3 files. Stomatal complexes oriented with their long axes perpendicular to the lateral veins or in some cases slightly oblique. Each stomatal complex consisting of a pair of guard cells flanked by two subsidiary cells. Stomatal density ca 36–50 complexes per square mm. Trichomes and trichome bases sparse and scattered on abaxial side of leaf lamina only. Trichome bases one-celled.

Holotype. MPCFL–145/1–1; Pl. 7, fig. 1.

Other material. MPCFL–145/1–2 to MPCFL–145/1–5, PP56997, PP57006; Pl. 7, figs 2–6, Pl. 8, Pl. 9, Pl. 10, fig. 6.

Repository. Mongolian Paleontological Center, Ulaanbaatar, Mongolia (specimens with prefix MPCFL), Paleobotanical Collections, Department of Geology, The Field Museum, Chicago, Illinois, USA (specimens with prefix PP).

Stratigraphic position and age. Khukhteeg Formation, Aptian–Albian stage (125–99.6 Mya), Early Cretaceous.

**Plate 4**. Early Cretaceous leaves of *Nilssoniopteris tomentosa* sp. nov. from Tevshiin Govi. SEM micrographs, light micrographs and line drawings of leaves. **1**. Abaxial surface of fragment of midrib, showing three-dimensionally preserved, densely tomentose covering of branched trichomes. Detail of outlined area shown in Plate 4, Fig. 3 (PP56992); **2**. Abaxial surface of leaf, showing midrib and lamina covered in dense tomentose trichomes; line drawing, showing midrib in grey (PP56992); **3**. Detail from Plate 4, Fig. 1 (outlined), showing dense covering of branched trichomes over midrib; **4**. Detail of dense covering of branched trichomes from leaf lamina. Detail of outlined area shown in Plate 4, Fig. 5 (PP56992); **5**. Detail from Plate 4, Fig. 4, showing branched trichome with multiple lateral branches. Note strongly flattened form; **6**. Isolated trichomes, showing spine-like tips of lateral branches; trichome at far right has been partially macerated to reveal the multicellular organization (PP56993). Scale bars = 1 mm (1, 2); 500 μm (3); 200 μm (4); 100 μm (5, 6)


**Plate 5**. Early Cretaceous bract-scales of *Cycadolepis* sp. from Tevshiin Govi. Light micrographs. **1**. Broadly ovate bract-scale with acuminate spine-like apex, showing adaxial (left) and abaxial surfaces (right). Note tightly intertwined, tomentose covering of trichomes on adaxial surface, while abaxial surface (right) has trichomes only near margin of scale (PP56994); **2**. Broadly ovate bract-scale with acuminate apex with rounded tip, showing adaxial (left) and abaxial surfaces (right). Note tightly intertwined, tomentose covering of trichomes on adaxial surface (right), while abaxial surface has trichomes only near margin of scale (PP56995). Scale bars = 2 mm

Locality. Shivee Ovoo coal mine (46°13′47.4″N, 108°54′8″E), central Mongolia.

Etymology. From Shivee Ovoo, where the fossils were found.

Detailed description. Leaves petiolate. Midrib stout, transversely striated to smooth, ca 1.5–3.5 mm wide (measured near base) (Pl. 7, figs 3–6). Leaf lamina at least ca 15–19 cm long and 1.4–2.0 cm wide. Lamina strongly elongate, narrow, strap-shaped, undivided (not subdivided into segments), and attached to adaxial surface of midrib, leaving part of upper surface of midrib exposed (Pl. 7, figs 1, 2). Lamina margin entire. Apex convex to slightly retuse, with midrib ending at tip (Pl. 7, fig. 3). Base symmetrical, convex to slightly cordate (Pl. 7, fig. 6). Numerous lateral, parallel veins entering lamina with density of ca 25–40 veins per cm in middle region of leaf to ca 30–50 veins per cm in proximal and distal regions. In basal leaf lamina, lateral veins commonly dichotomizing close to midrib; near middle and apex of leaf lamina, the lateral veins commonly dichotomizing near margin; lateral veins also unbranched (Pl. 7, figs 3–6); all lateral veins slightly curving exmedially just before ending at margin (Pl. 7, fig. 5). Rejoining of lateral veins extremely rare. Lateral veins inserted on midrib at ca 80–90° proximally, to 45–75° medially and distally. Lateral veins equal in thickness.

Midrib epidermal cells isodiametric, mostly square to rectangular in outline and arranged

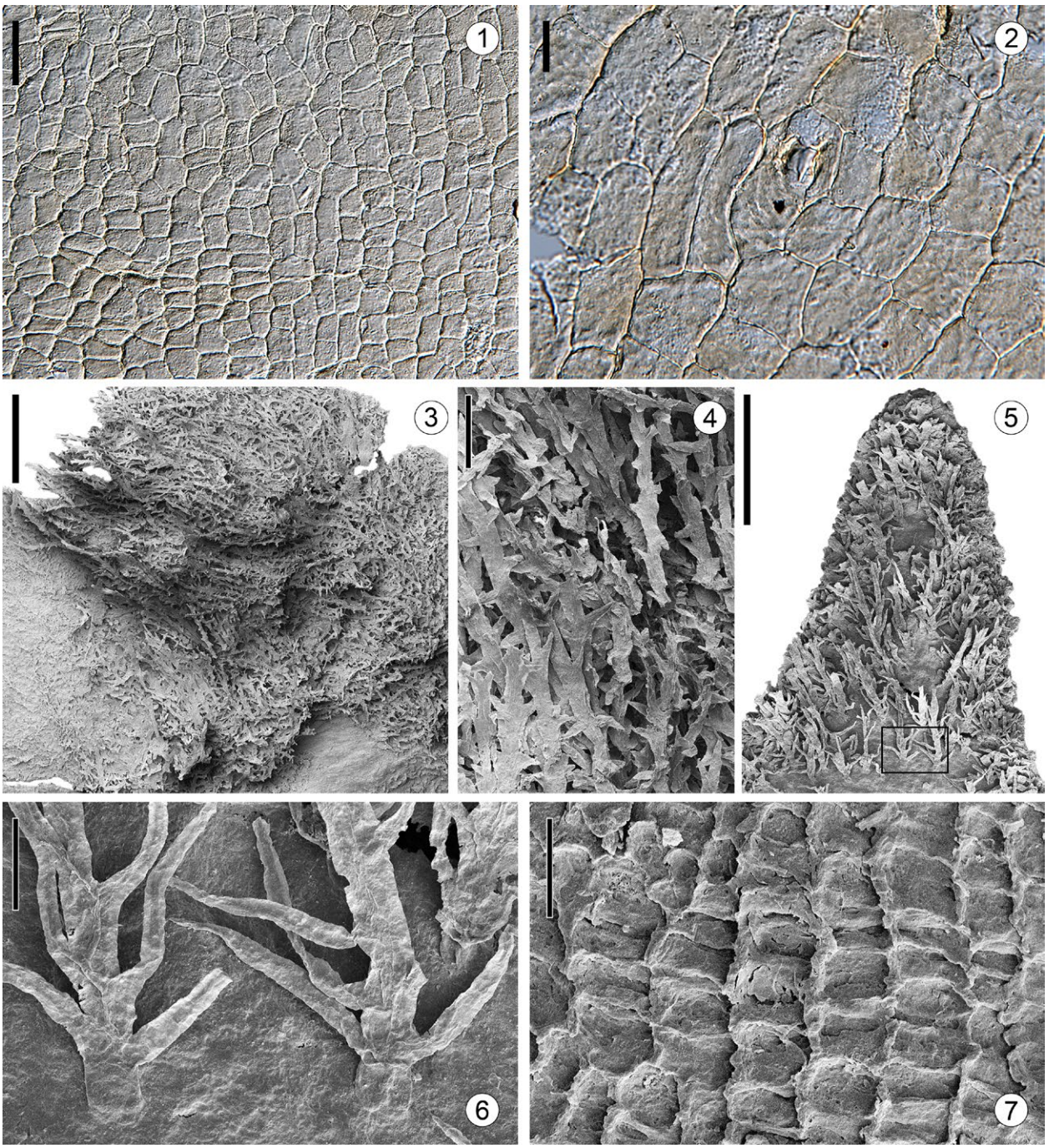


**Plate 6**. Early Cretaceous bract-scales of *Cycadolepis* sp. from Tevshiin Govi. Light and SEM micrographs. **1**. Presumed adaxial cuticle of bract-scale, showing square to polygonal epidermal cell outlines arranged in longitudinal files (PP56996); **2**. Presumed adaxial cuticle of bract-scale, showing a single brachyparacytic (syndetocheilic) stomatal complex (PP56996); **3**. Detail of adaxial surface of bract-scale from Plate 5, Fig. 1 (left), showing dense, tomentose covering of trichomes (PP56994); **4**. Detail from Plate 6, Fig. 3, showing cluster of branched and flattened trichomes; **5**. Detail of abaxial surface from Plate 5, Fig. 2 (right), showing tomentose covering of trichomes near apex of bract-scale; most apices of trichomes appear broken. Outlined area shown in Plate 6, Fig. 6. (PP56995); **6**. Detail from Plate 6, Fig. 5 (outlined), showing trichome bases and spiny lateral branches of three trichomes. Note circular trichome bases and flattened form of trichomes; **7**. Presumed abaxial cuticle of bract-scale, showing square to polygonal epidermal cells arranged in longitudinal files (PP56995). Scale bars = 1 mm (3); 500 µm (5); 200 µm (4); 50 µm (1, 6, 7); 20 µm (2)

in longitudinal files on both adaxial and abaxial cuticle (Pl. 8, fig. 1, Pl. 9, figs 1, 2). Square to nearly square cells ranging from 30 to 44 µm; rectangular to more longitudinally elongated cells 17–40 µm wide and 54–105 µm long. Upper surface of midrib with stomata. Trichome bases abundant on abaxial side of midrib, measuring ca 9–20 µm in diameter (Pl. 8, fig. 1, Pl. 9, figs 1, 2). Periclinal walls finely striate. Anticlinal walls moderately to strongly sinuous.

Leaf hypostomatic. Cuticles of both adaxial and abaxial leaf surfaces thick and well

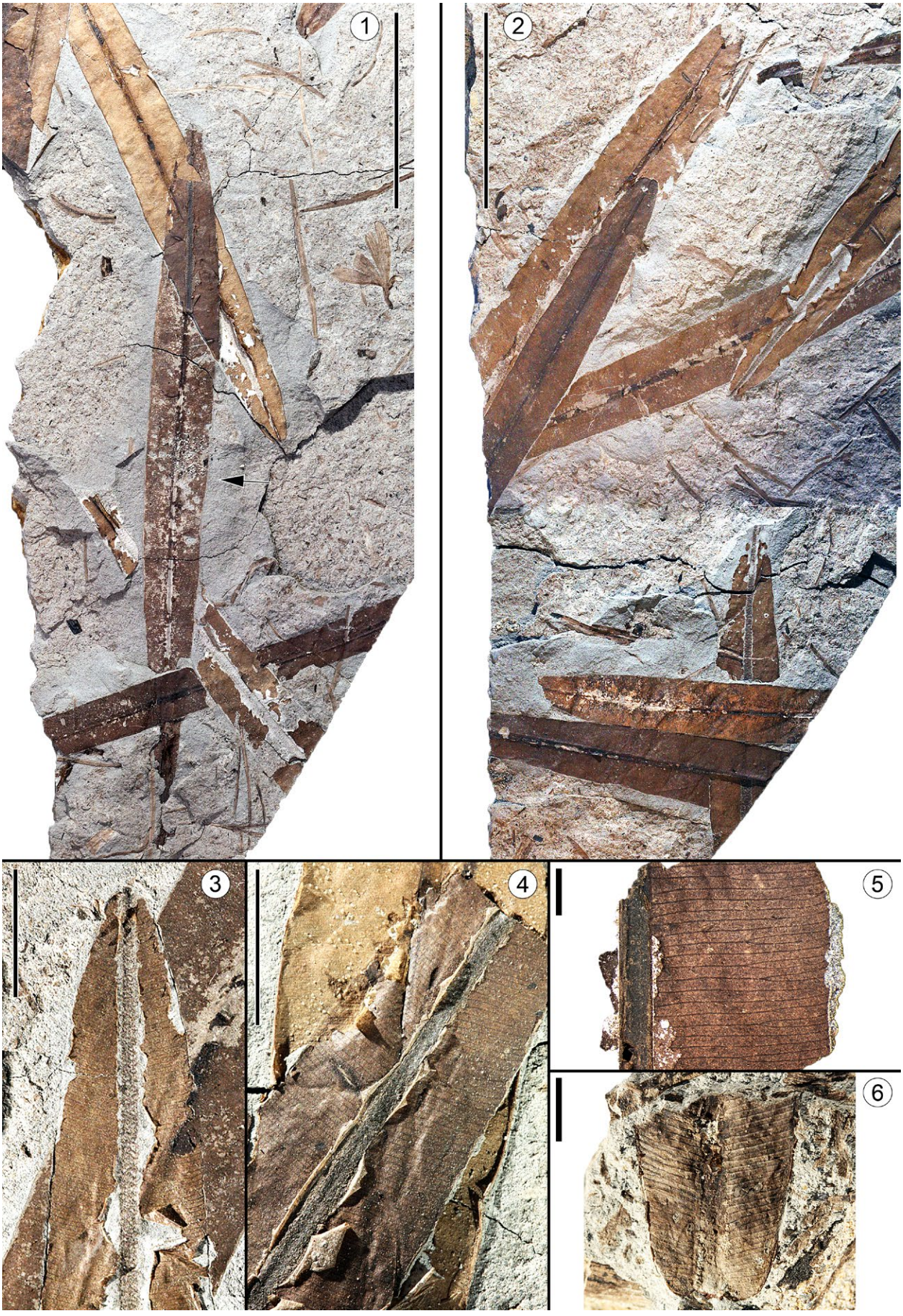
1
2
3
4
5
6

preserved. Adaxial leaf surface lacking stomata, consisting almost entirely of rectangular epidermal cell outlines, 44–92 µm long and 15–32 µm wide (Pl. 9, fig. 3). Periclinal walls consistently finely granular. Outer surface of adaxial cuticle lacking papillae, trichomes or hair bases. Anticlinal walls well cutinized with uneven thickenings and strongly sinuous with widely spaced folds (Ω-shaped; Pl. 9, fig. 3). Abaxial cuticle consisting of epidermal cells, usually rectangular to square in outline, 40–72 µm long and 20–37 µm wide (Pl. 8, figs 2–4, Pl. 9, figs 4, 5). Periclinal walls smooth to finely granular. Anticlinal walls well cutinized, with uneven thickenings, strongly sinuous with widely spaced folds (Ω-shaped). Abaxial leaf surface with trichomes bases on outer cuticular surface (see description below).

Abaxial leaf surface with brachyparacytic (syndetocheilic) stomatal complexes (Pl. 8, figs 2–6, Pl. 9, figs 4–7) arranged in poorly defined irregular bands composed of one to three files, ca 125–200 µm wide. Stomatal bands oriented parallel to lateral veins, one band between two lateral veins (Pl. 8, fig. 2, Pl. 9, figs 4, 5, Fig. 1B). Stomatal complexes oriented with their long axes perpendicular to the lateral veins, but also oblique and rarely parallel to the veins, at ca 5–65° (Pl. 8, fig. 2, Pl. 9, figs 4–7, Fig. 1B). Stomatal density ca 36–50 complexes per square mm. Stomatal complexes crowded to widely spaced but never directly sharing lateral subsidiary cells; stomatal complexes occurring ± isolated within stomatal band and separated by one or two normal epidermal cells (Pl. 8, figs 3–6, Pl. 9, figs 4–7).

Stomatal complexes ca 24–34 µm long (distance between polar walls of guard cells) and 37–44 µm wide (distance between outermost walls of lateral subsidiary cells), ± elliptical in outline. Stomatal complexes sunken, each consisting of a pair of guard cells with two subsidiary cells (Pl. 8, figs 5, 6, Pl. 9, figs 6, 7). Stomatal aperture slit-like, oriented parallel to lateral subsidiary cells and flanked by two heavily cutinized lips (5.6–6.8 µm long, 1.3–2.2 µm wide). Cuticular flanges between guard cells and subsidiary cells strongly developed and butterfly-shaped (Pl. 9, figs 6, 7). Guard cells 17–23 µm long, 6–10 µm wide, crescent-shaped in outline, sunken, with strongly cutinized dorsal thickenings and polar extensions, commonly of unequal lengths in the same stomatal complex. Guard cells flanked by two lateral subsidiary cells 23–32 µm long, 14–19 µm wide (Pl. 8, figs 5, 6, Pl. 9, figs 6, 7). Subsidiary cells visible, with flange of outer wall irregular serrate or sinuous to convex, symmetrical or asymmetrical in outline, oriented parallel to stomatal aperture and extending beyond the length of guard cells. Outer surface of cuticle over guard cells and subsidiary cells finely granular and without papillae.

Trichome bases present only on abaxial leaf cuticle, including in stomatal bands and over veins. Trichome bases unicellular, widely spaced, 12–27 µm in diameter, elliptical to rounded in outline, with sinuous and tightly folded thickened margin (Pl. 8, figs 3, 4, Pl. 10, fig. 6). Trichome density ca 12–18 bases per square mm.

## DISCUSSION

### ASSIGNMENT TO *NILSSONIOPTERIS* AND COMPARISON OF MONGOLIAN FOSSILS

Both leaf fossils described here are assigned to the genus *Nilssoniopteris* based on their petiolate, strap-shaped form with an undivided lamina that is attached toward the adaxial surface of the midrib. Also consistent with assignment to *Nilssoniopteris* is the pattern of venation and epidermal structure. Abundant lateral veins, which may remain unbranched, dichotomize or rarely rejoin to form simple anastomoses, diverge from the midrib typically at 70–90°, and end at the leaf margin. Stomatal complexes are syndetocheilic, and the outlines of the epidermal cells on both the abaxial and adaxial cuticles are strongly sinuous (Ω-shaped). Taken in combination, these characters are diagnostic

**Plate 7**. Early Cretaceous leaves of *Nilssoniopteris shiveeovoensis* sp. nov. from Shivee Ovoo. Light micrographs of leaf macrofossils. **1**. Block of sediment, showing several elongate, strap-shaped leaves. Holotype (MPCFL–145/1–1) indicated by arrow; **2**. Block of sediment, showing fragments of several elongate and strap-shaped leaves; note stout midribs. Note lamina tapering gradually toward leaf apex and base (MPCFL–145/1–2); **3**. Detail of leaf, showing stout midrib and slightly retuse apex (MPCFL–145/1–3); **4**. Detail of leaf, showing stout midrib and abundant lateral veins. Note well-preserved cuticle (MPCFL–145/1–4); **5**. Leaf fragment, showing lateral veins, some of which dichotomize toward leaf margin and one of which apparently rejoins after dichotomizing to form a simple aberrant anastomosis (PP56997). This fragment was macerated for cuticular analysis (Pl. 8, 9); **6**. Leaf fragment, showing basal part of lamina with stout midrib, lateral veins, and slightly cordate base (MPCFL–145/1–5). Scale bars = 5 cm (1, 2); 1 cm (3, 4); 5 mm (6); 2 mm (5)

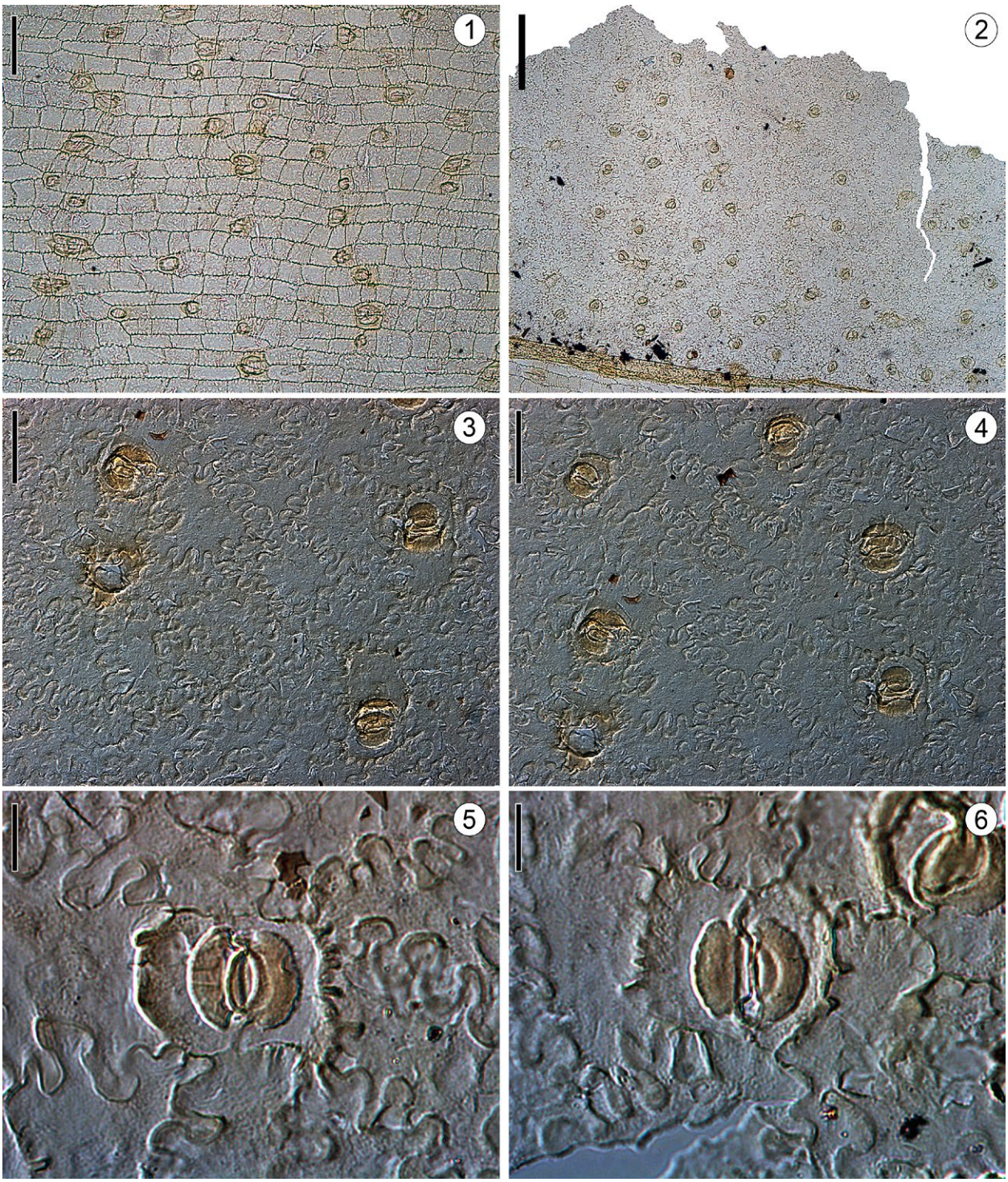


**Plate 8**. Early Cretaceous leaves of *Nilssoniopteris shiveeovoensis* sp. nov. from Shivee Ovoo. Light micrographs of leaf cuticles and stomata (PP56997). **1**. Abaxial cuticle of midrib (oriented horizontally), showing elongate rectangular to square epidermal cell outlines arranged in longitudinal files; note abundant trichome bases, each of which arises from the center of a single epidermal cell; **2**. Abaxial cuticle of leaf lamina (oriented vertically), showing arrangement of stomata and trichome bases; note at least three poorly defined stomatal bands (see Fig. 1); **3**. Abaxial cuticle of leaf lamina, showing epidermal cell outlines with sinuous anticlinal walls, three stomata with prominently cutinized guard cell thickenings, and one trichome base; **4**. Abaxial cuticle of leaf lamina, showing epidermal cell outlines with sinuous anticlinal walls, five stomata with prominently cutinized guard cell thickenings, and one trichome base; **5**. Detail of abaxial cuticle, showing strongly sinuous epidermal cell outlines and a brachyparacytic (syndetocheilic) stomatal complex. Note clearly differentiated subsidiary cells and prominent cuticular thickenings of pair of guard cells; **6**. Detail of abaxial cuticle, showing strongly sinuous epidermal cell outlines and brachyparacytic (syndetocheilic) stomatal complex. Note clearly differentiated subsidiary cells and prominent cuticular thickenings of pair of guard cells. Scale bars = 200 µm (2); 40 µm (1, 3, 4); 20 µm (5, 6)

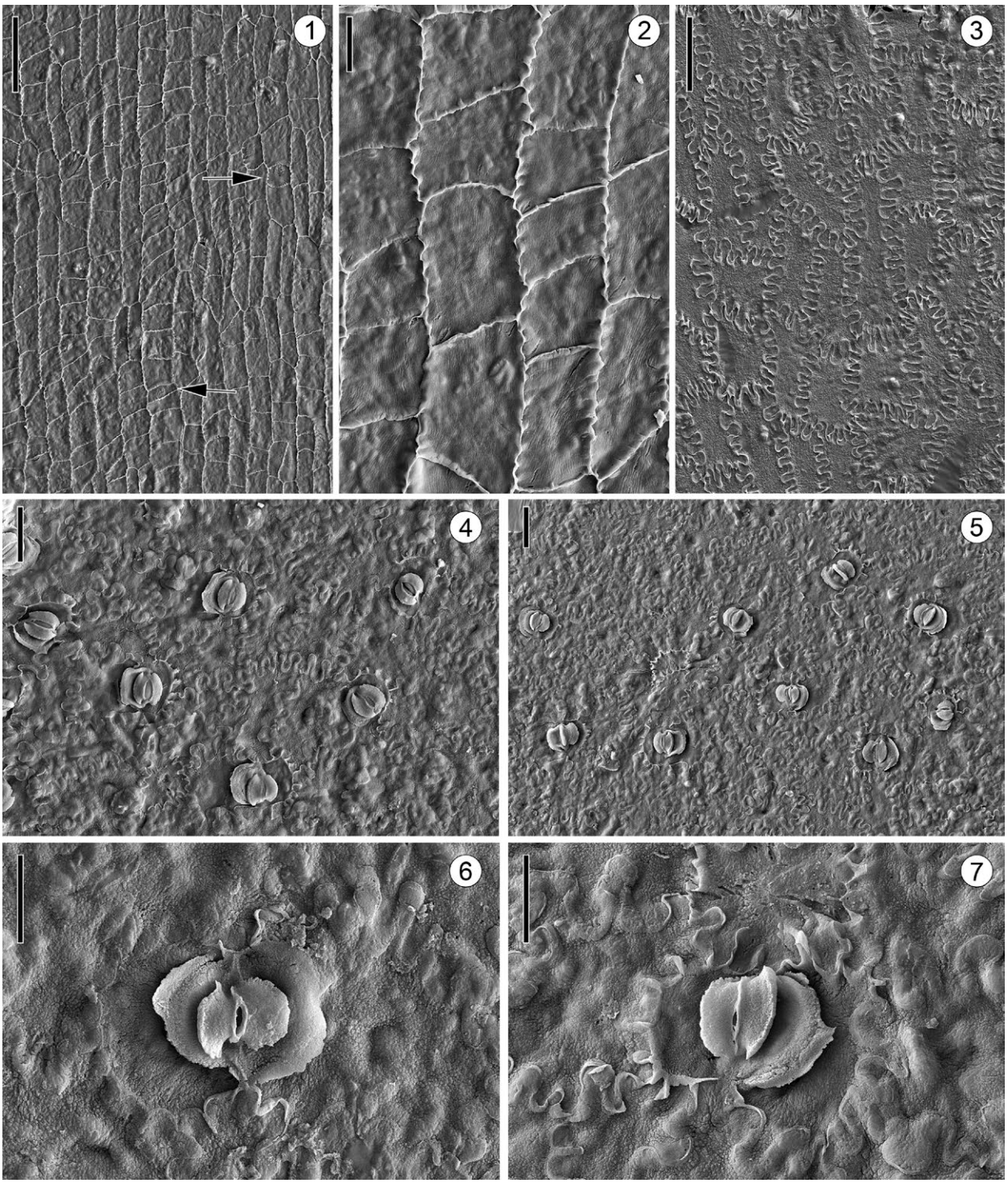


**Plate 9**. Early Cretaceous leaves of *Nilssoniopteris shiveeovoensis* sp. nov. from Shivee Ovoo. SEM micrographs of inner surface of leaf cuticles and stomata (PP56997). 1. Inner surface of abaxial cuticle of midrib, showing elongate rectangular to square epidermal cell outlines arranged in longitudinal files. Note occasional sparse trichome bases (arrows); **2**. Detail from Plate 9, Fig. 1, showing finely striate periclinal walls and slightly sinuous outlines of anticlinal cell walls; **3**. Inner surface of adaxial cuticle, showing epidermal cell outlines demarcated by well-cutinized, strongly sinuous and widely spaced folds of anticlinal flanges; **4**. Inner surface of abaxial cuticle, showing epidermal cell outlines with strongly sinuous walls and six brachyparacytic (syndetocheilic) stomatal complexes. Note the pronounced and often asymmetric thickening of the periclinal wall of one of the two subsidiary cells; **5**. Inner surface of abaxial cuticle, showing epidermal cell outlines with strongly sinuous walls and nine brachyparacytic (syndetocheilic) stomatal complexes; **6**. Inner surface of abaxial cuticle, showing detail of stoma with pair of guard cells with two subsidiary cells; **7**. Inner surface of abaxial cuticle, showing detail of stoma; note crescent-shaped, strongly cutinized thickenings of guard cells. Note the pronounced asymmetric thickening of the periclinal wall of one of the two subsidiary cells. Scale bars = 100 μm (1); 40 μm (3, 4, 5); 20 μm (2, 6, 7)

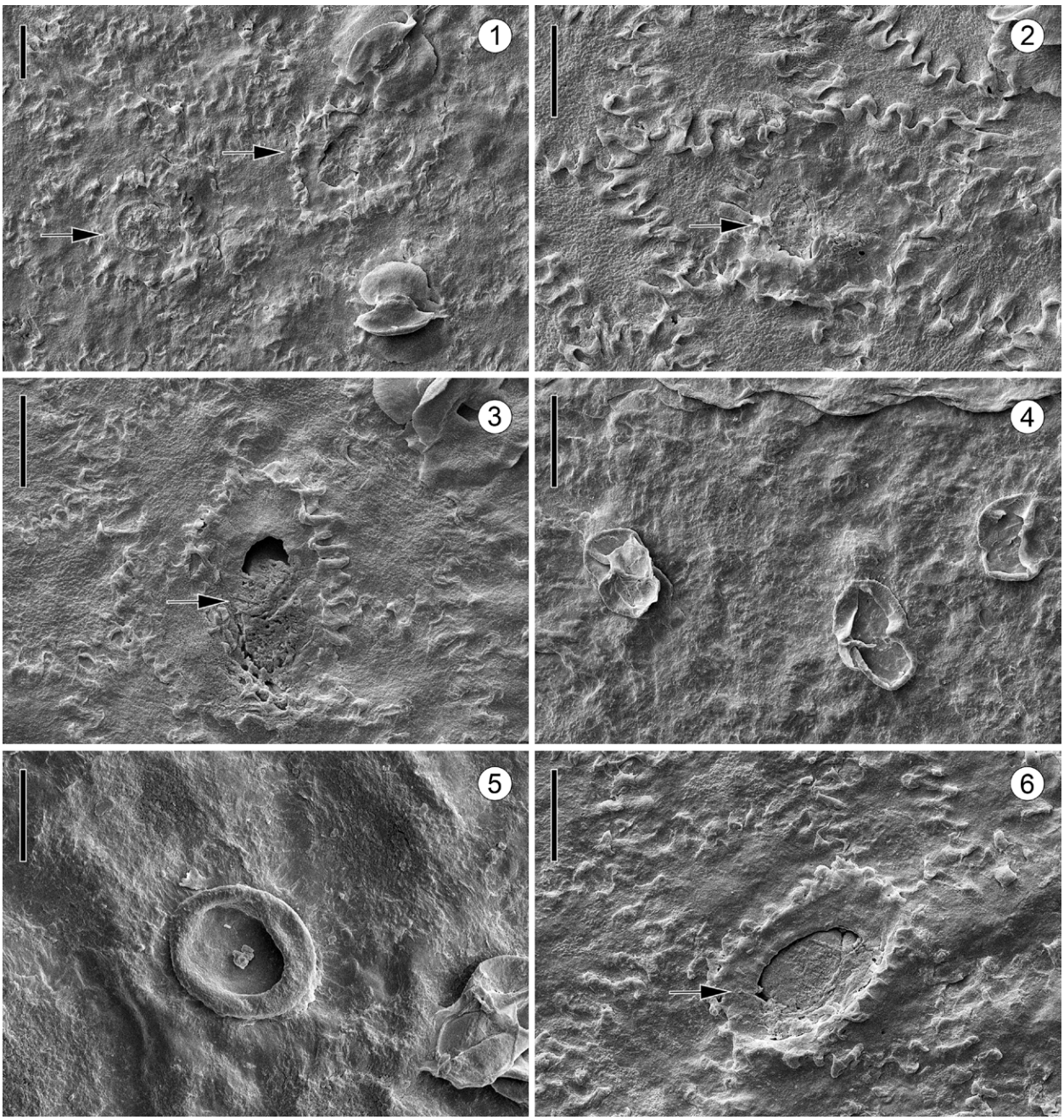


**Plate 10**. Leaves of *Nilssoniopteris tomentosa* sp. nov. from Tevshiin Govi (1–5) and *Nilssoniopteris shiveeovoensis* sp. nov. from Shivee Ovoo (6). SEM micrographs of trichome bases; **1**. Inner surface of abaxial cuticle, showing two stomata, strongly sinuous epidermal cell outlines, and two trichome bases (arrows). Note that both trichome bases are in the center of the outline of normal epidermal cells (PP56991); **2**. Inner surface of abaxial cuticle, showing strongly sinuous epidermal cell outlines and two-celled trichome base in the center of the outline of a normal epidermal cell (arrow) (PP56991); **3**. Inner surface of abaxial cuticle, showing strongly sinuous epidermal cell outlines and two-celled trichome base in the center of the outline of a normal epidermal cell (arrow) (PP56991); **4**. Outer surface of abaxial cuticle, showing three trichome bases, all of which appear to have two-celled base (PP56998); **5**. Outer surface of abaxial cuticle, showing a trichome base with single-celled base (PP56998); **6**. Inner surface of abaxial cuticle of *Nilssoniopteris shiveeovoensis* sp. nov**.,** showing trichome base composed of a single cell arising in the center of the outline of a normal epidermal cell (arrow) (PP56997)

of the genus *Nilssoniopteris* (e.g. Boyd 2000, Cleal et al. 2006, Pott et al. 2007, Van Konijnenburg-van Cittert et al. 2017, Zhao et al. 2018).

The two new *Nilssoniopteris* taxa are similar in leaf shape, margin, venation and cuticular features. However, *N. tomentosa* from Tevshiin Govi is distinguished from *N. shiveeovoensis* from Shivee Ovoo by its much smaller size [at least 2.8 cm long (estimated complete length 5–6 cm long) and 0.8–1.5 wide vs. at least 15–19 cm long and 1.4–2.0 cm wide] as well as differences in the density and distribution of stomata and trichome bases. In *N. tomentosa* the stomatal bands are ca 145–320 μm

wide and composed of 2–4 files of stomata. In *N. shiveeovoensis* the stomatal bands are ca 125–200 μm wide and composed of 1–3 files of stomata (Fig. 1). In addition, in *N. tomentosa* each subsidiary cell bears a single, large, solid papilla that overarches the stomatal aperture, which appear to be absent in *N. shiveeovoensis*. The two species also differ in the density of stomata and trichome bases. In *N. tomentosa* the stomata are very numerous (ca 65–82 stomatal complexes per square mm), whereas in *N. shiveeovoensis* the stomata are scattered and less abundant (ca 36–50 complexes per square mm: Pl. 3, fig. 5, Pl. 9, fig. 5, Fig. 1). In *N. tomentosa* the trichome bases consist of one or two cells and are extremely abundant (ca 72–95 trichome bases per square mm), whereas in *N. shiveeovoensis* the trichome bases are scattered and exclusively unicellular (ca 12–18 trichome bases per square mm) (Pl. 10, Fig. 1).

Krassilov (1982) recognized from Mongolia six different kinds of Early Cretaceous bennettitalean leaves and bract-scales based on compression/impression fossils: *Nilssoniopteris denticulata*, *Otozamites lacustris*, *Otozamites* sp., *Neozamites verchojanicus* Vakhram, *Pterophyllum* spp. and *Cycadolepis* sp. Among these, *Nilssoniopteris denticulata* Krassilov, described from the Bon-Tsagan, Shin-Khuduk and Modon-Usu localities, is most similar to the two taxa reported here, but is distinct in having small but unusually well-developed teeth on the leaf margin. There are also no indications of trichomes or trichome bases in Krassilov's description, drawings or photographs of *N. denticulata*.

More similar with regard to the presence of trichomes is the single impression specimen from Bon-Tsagan described as *Cycadolepis* sp. by Krassilov (1982). The bract-scale is ca 21 mm long and 10 mm wide, with a conspicuous emarginate apex. Our reexamination of this compression specimen confirms Krassilov's interpretation; the bract has abundant unbranched trichomes near the base as well as along the upper margin. However, the *Cycadolepis* bract from Tevshiin Govi differs from the Bon-Tsagan specimen in its smaller size (6.6–9.5 mm long), its acuminate and spine-like apex, and its abundant, conspicuously branched trichomes.

## COMPARISON WITH OTHER *NILSSONIOPTERIS* SPECIES

Dozens of *Nilssoniopteris* species have been reported from Late Triassic to Late Cretaceous deposits, especially from Northern Hemisphere localities (e.g. Nathorst 1909, Harris 1926, Florin 1933, Krassilov 1967, Zhang et al. 1980, Zheng & Zhang 1982, Wang 1984, Li

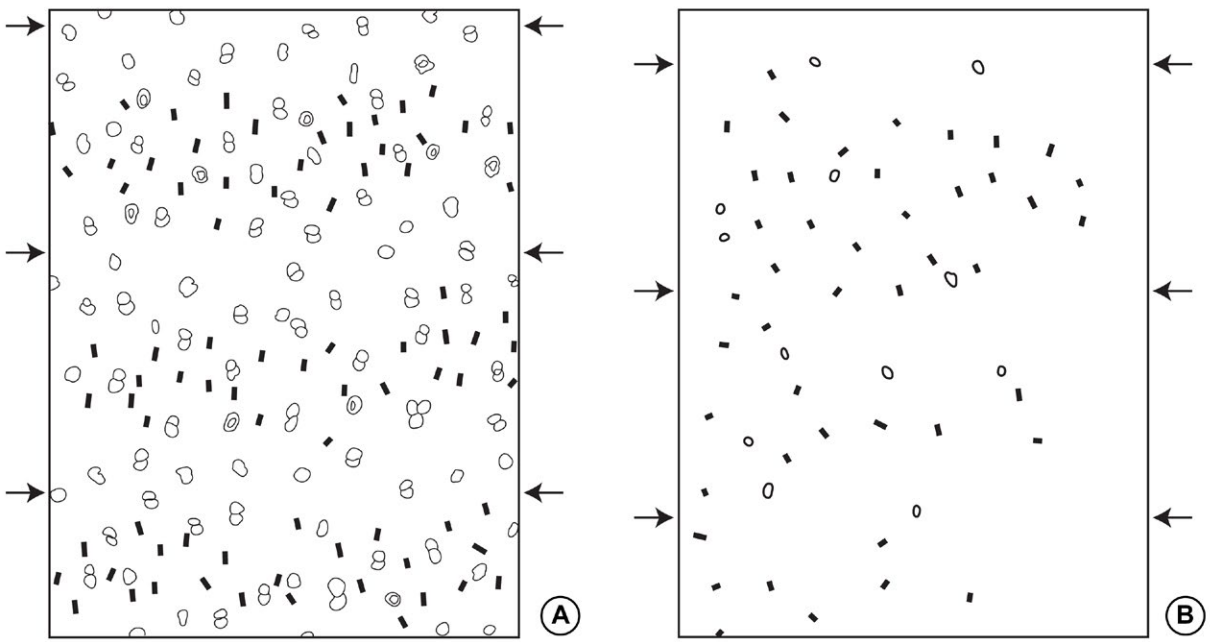


**Fig. 1**. Distribution and orientation of stomata and trichome bases on leaf laminae of *Nilssoniopteris tomentosa* sp. nov. from Tevshiin Govi (A) and *Nilssoniopteris shiveeovoensis* sp. nov. from Shivee Ovoo (B). Solid dark lines indicate orientation of stomatal apertures; open elliptical shapes indicate trichome bases; arrows indicate position of lateral veins running perpendicular to midrib

et al. 1986, Chen et al. 1988, Sun & Shen 1988, Wu 1988, 1993, Zhou 1989, Manum et al. 1991, Deng 1995, Deng et al. 1997, Barale et al. 1998, Boyd 2000, Schweitzer & Kirchner 2003, Pott et al. 2007, 2010, 2016, Crane & Herendeen 2009, Na et al. 2014, Ray et al. 2014, Pott & Van Konijnenburg-Van Cittert 2017, Zhao et al. 2018: see also the extensive comparative tables of *Nilssoniopteris* taxa compiled by Na et al. 2014 and Ray et al. 2014). *Nilssoniopteris tomentosa* and *N. shiveeovoensis* can clearly be distinguished from all these previously described *Nilssoniopteris* leaves.

Of particular interest for comparison with the Mongolian fossils are those Jurassic and Early Cretaceous species of *Nilssoniopteris* reported from Eastern Asia and Western North America. Four Early Cretaceous species of *Nilssoniopteris* that are similar in size and shape to *N. shiveeovoensis* were reported from sediments in the Changcai Coal Mine in Jilin, NE China (Wei et al. 2005). Of these, *N. prynadae* Samylina, *N. longifolia* Doludenko? and *Nilssoniopteris* sp. all lack trichome bases, as is also the case in *N. binggouensis* Na, C. Sun, Dilcher et Hongshan Wang (Na et al. 2014) from western Liaoning Province, China. Trichome bases were only reported in *N. paltyrachis* (Samylina) W. Wei from the Changcai region, but this species has cuticles with abundant papillae on the periclinal walls of the epidermal cells. *Nilssoniopteris hailarensis*, also Early Cretaceous, from northeastern China, Yimin Formation (Zheng et al. 1990), is distinguished from the new Mongolian fossils by its very narrow lamina (5–6 mm wide), broad midrib (up to 3 mm wide) and low stomatal density (20–25 complexes per square mm).

The Early Cretaceous *N. amurensis* (Novopokr.) Krassilov (Krassilov 1973) from the Bureja basin in the Russian Far East is especially important for comparison with the two Mongolian species because of the several taxa shared between the Bureja (Markevich & Bugdaeva 2014) and Tevshiin Govi floras (e.g. *Elatides*, *Podozamites*, *Pseudotorellia*, and *Umaltolepis*). However, *Nilssoniopteris amurensis* is very distinct in its amphistomatic leaves which lack abaxial trichomes. The two anatomically preserved Early Cretaceous *Nilssoniopteris* leaves are difficult to compare with the two new Mongolian taxa (Yamada et al. 2009, Ray et al. 2014). However, *N. oishii* from the Barremian Arida Formation of Japan can be distinguished from *N. tomentosa* and *N. shiveeovoensis* on the basis of its segmented lamina and predominantly unbranched lateral veins (Yamada et al. 2009). *Nilssoniopteris corrugata* from the Valanginian Apple Bay flora, British Columbia, Canada, differs from both new leaf taxa from Mongolia by its apparent lack of abaxial trichomes and the rarely dichotomous lateral veins.

Among the several species of *Nilssoniopteris* leaves described from Jurassic floras from Eastern Asia (see Na et al. 2014, Ray et al. 2014, Zhao et al. 2018), *N. neimenguensis* (Early Jurassic) from the Hongqi Formation, Xilinhot Basin, central Inner Mongolia, China (Deng et al. 2017), is similar to *N. shiveeovoensis* in its elongated strap-shaped leaves (> 8 cm in length; Deng et al. 2017) but differs from both *N. shiveeovoensis* and *N. tomentosa* in its low density of lateral veins (ca 18–20 per cm), the presence of adaxial trichomes, and subsidiary cells which bear papillae-like spines. Interestingly, lateral veins also occur at low density in several other *Nilssoniopteris* species from the Jurassic of Asia. *Nilssoniopteris inconstans* (Middle Jurassic) from the Yaojie Formation, Lanzhou, Gansu, China (Sun & Shen 1988), contrasts with *N. tomentosa* and *N. shiveeovoensis* primarily due to its segmented lamina as well as low lateral vein density (ca 18–20 per cm). Also from China, *Nilssoniopteris* sp. from the Jurassic Xiangxi Formation, western Hubei (Sun & Yang 1988), contrasts with both Mongolian species by its linear, strap-shaped leaf and low lateral-vein density (ca 16–20 per cm). *Nilssoniopteris bolei* (Middle Jurassic) from the Yima Formation, Henan, central China (Barale et al. 1998), differs from the new species by the combination of its oval-lanceolate leaf shape, low lateral vein density (ca 21–24 per cm) and sparse trichome bases. Two other Middle Jurassic *Nilssoniopteris* species – *N. hamiensis* and *N. crassiaxis* from the Xishanyao Formation, Xinjiang, China (Zhao et al. 2018) – differ from both Mongolian leaves mainly in having lateral veins that vary from simple and free to dichotomous to trichotomous and that also commonly merge to form anastomoses.

## PALAEOECOLOGICAL CONSIDERATIONS

Bennettitalean plants included palm-like, pachycaulous and slender trees or shrubs that were widespread during the Mesozoic, and

there is increasing evidence that these plants were mainly early successional shrubs of open habitats (Krassilov 1981). As in *Nilssoniopteris tomentosa* (microphyll) and *N. shiveeovoensis* (small mesophyll), bennettitalean leaves are typically microphylls or small mesophylls (e.g. Harris 1969, Watson & Sincock 1992, Boyd 2000). Seeds in Bennettitales were also small, consistent with an early successional role and germination in open rather than shaded habitats (Harper et al. 1970, Harris 1973). Notably, even in the slender-branched Bennettitales the stems were relatively thick in relation to the size of leaves, which is often characteristic of plants that are shade-intolerant (White 1983). The divaricate habit of some of these taxa may also indicate growth in open vegetation communities on nutrient-deficient soils (Pott & McLoughlin 2014), and to the extent that pinnate bennettitalean leaves are similar to compound leaves in angiosperms they also conform to morphologies that theoretically are more advantageous for early successional rather than climax forest trees (Givnish 1978).

It has also been inferred that leaf mass per area was lower in Bennettitales than in all extant woody seed plants (Soh et al. 2017) and that the turnover of bennettitalean leaves (leaf life span) was relatively rapid, with higher leaf nitrogen concentrations and higher maximum photosynthetic rates than in coeval seed plants such as Ginkgoales (Soh et al. 2017). Based on stomata, maximum stomatal and canopy transpirational rates have been estimated as 40% higher than Ginkgoales (Steinthorsdottir et al. 2012). This implies that to maintain their higher photosynthetic rates the Bennettitales may have had greater demands for water and nitrogen (Soh et al. 2017). Growth as early successional plants of open environments, combined with significant demands for water and nitrogen, may partially explain the xeromorphic features of many bennettitalean leaves (reflexed pinnae, well-developed abaxial hairs or papillae, sunken stomata, stomata partly occluded by epidermal papillae; e.g. Harris 1969). The size, morphology and anatomy of *N. tomentosa* and *N. shiveeovoensis*, with flat leaves, well-developed cuticles, sunken stomata that are partly occluded, and an indumentum on the abaxial surface, is consistent with this emerging picture of Bennettitales as plants of open habitats that often grew under conditions of water stress.

*Nilssoniopteris tomentosa* is rare in the Tevshiin Govi flora and does not occur in the widespread peat-swamp vegetation that produced the Tevshiin Govi lignite (Herrera et al. 2015). Nevertheless, most of the plants with which the Bennettitales leaves co-occur, such as the cones of the archaic conifer *Krassilovia* (Herrera et al. 2015), the ginkgophyte *Umaltolepis* (Herrera et al. 2017b) and the leaves of *Podozamites* and *Pseudotorellia* (Shi et al. 2018), also occur in the lignite, and the few taxa encountered for the first time in the channel flora [two new *Umkomasia* cupules (Shi et al. in press) and one new *Schizolepidopsis* species] are very similar to species that occur in the lignite. In both the peat-swamp and the channel flora all leaves are microphyllous or smaller (i.e. Leslie et al. 2014, Herrera et al. 2016, Herrera et al. 2017a, Shi et al. 2018). Based on comparisons with modern peat swamps in which the vegetation grows in waterlogged conditions, small leaf size suggests high light and low nutrient conditions (Aribal et al. 2017). Under these conditions, sustaining high photosynthetic rates would have required efficient water use; the well-developed indumentum on the leaves of *N. tomentosa* may reflect an adaptation of this kind. The plants that produced the leaves of *N. shiveeovoensis* grew under more favorable conditions on better-drained parts of the floodplain. Leaves of *N. shiveeovoensis* are larger, stomata per unit area are fewer, and the density of hairs (judged from hair bases) is much lower. The implication is that conditions for growth were significantly better than in or near the swamps, with better-drained soils, more readily available nutrients, and adequate water.

The type species of the genus *Nilssoniopteris*, *N. tenuinervis* (Nath.) Nath. from the Middle Jurassic of Yorkshire, U.K. (Cleal & Rees 2003, Cleal et al. 2006, Pott et al. 2007, Van Konijnenburg-van Cittert et al. 2017, Zhao et al. 2018), appears to lack trichomes or trichome bases, but these are very common among other *Nilssoniopteris* species (see Na et al. 2014, Ray et al. 2014) as well as in other genera of bennettitalean leaves (e.g. Sincock & Watson 1988, Watson & Sincock 1992, Boyd 2000, Gordenko & Broushkin 2010, Pott et al. 2012). The trichome bases are typically one- or two-celled (rarely three-celled or more) and may be very sparse or abundant, and all appear very similar in morphology at high magnification under SEM (e.g. *N. pecinovensis*; Kvaček 1995). Of

the 49 *Nilssoniopteris* taxa listed by Ray et al. (2014), 24 preserved abaxial trichome bases, 15 appeared to lack them, and in 10 no data were available.

While trichome bases are a common feature of bennettitalean leaves, the trichomes themselves are preserved only rarely. Nevertheless, the sparse evidence available suggests that trichomes were relatively morphologically diverse within the group. A few specimens of *Nilssoniopteris major* from the Middle Jurassic Yorkshire flora (Harris 1969) show a thin covering of stellate hairs, preserved as impressions in the matrix and on the cuticles. The hairs are up to 300 µm long, irregularly branched, and with 3 to 5 tapering points. Impression fossil leaves of the Middle Jurassic *Anomozamites villosus* from the Daohugou flora of Inner Mongolia, China (Pott et al. 2012), also show that the margins and abaxial side of the rachis were densely covered with unicellular, long stiff hairs, while the abaxial laminar surface was thickly protected with soft shaggy hairs. The new Mongolian species *N. tomentosa* and its associated *Cycadolepis* sp. bract-scales show multicellular, distinctly flattened, and branched trichomes (Pl. 4, Pl. 6, figs 3–6). To our knowledge, similar morphological diversity of trichomes does not occur in any living gymnosperm, and occurs today only in angiosperms and ferns (e.g. Tryon 1965, Werker 2000, Evert 2006, Barthlott et al. 2010).

The rarity with which trichomes, as opposed to trichome bases, are preserved in compression fossils of *Nilssoniopteris* suggests low preservation potential. It is possible that the trichomes were deciduous, but in some cases trichomes could also have been lost during preparation of the cuticles. We noticed that the trichomes of *N. tomentosa* completely disappeared after more than five minutes of soaking in diluted sodium hypochlorite (Pl. 4, fig. 6). It is clear that the trichomes of *N. tomentosa* lacked a well-developed cuticle.

While the primary advantage of trichomes in bennettitalean leaves may have been to increase water use efficiency, trichomes in extant plants may also be important in temperature regulation, facilitating the condensation of moisture (Fahn 1986, Fahn & Cutler 1992, Dunkić et al. 2001, Wood 2005, Evert 2006, Cutler et al. 2007) and deterring insect herbivory (Levin 1973, Johnson 1975, Werker 2000, Dalin et al. 2008, War et al. 2012, Tozin et al. 2016). Among fossils, trichomes on leaves of *Anomozamites villosus* from the Middle Jurassic of China have been suggested as conferring protection from arthropod herbivory (Pott et al. 2012). Whether the trichomes of Bennettitales had this or other functions, in addition to their likely role in increasing water use efficiency, remains to be determined. It is interesting, however, that among the fossil plants recovered from Tevshiin Govi, *N. tomentosa* shows the most obvious evidence of insect damage, but the abundant gall scars are confined to the adaxial (Pl. 1, fig. 6) rather than the tomentose abaxial leaf surface.

ACKNOWLEDGEMENTS

We thank O. Nyamsambuu for assistance with fieldwork in Mongolia, B. Strack for assistance with scanning electron microscopy, and A. Busier, S. Crane and N. Gavin-Smyth for help selecting fossil material. E. Bugdaeva kindly provided photographs and allowed us the examine specimens collected by V.A Krassilov in Mongolia. We also thank C. Labandeira and M. Carvalho for comments on insect damage on the fossil leaves. F. Herrera thanks B. Himschoot for constant support. Funding for this work was provided by National Science Foundation Grants (DEB-1348456 to P.S.H. and P.R.C.; DEB-1748286 to P.S.H., P.R.C. and F.H.), the Oak Spring Garden Foundation (to F.H.) and Grants-in-Aid for Scientific Research (21405010 and 24405015) from the Japan Society for the Promotion of Science (to M.T.). We thank B. Bomfleur and a second anonymous reviewer for their helpful comments.

## REFERENCES

ARIBAL L.G., BONGGAY J.G. & FERNANDO E.S. 2017. Leaf size indices and structure of the peat swamp forest. Global J. Environ. Sci. Manage., 3(1): 63–74.

BARALE G., THÉVENARD F. & ZHOU Z.Y. 1998. Discovery of *Nilssoniopteris* in the Middle Jurassic Yima Formation of Henan, central China. Geobios, 31: 13–20.

BARTHLOTT W., SCHIMMEL T., WIERSCH S., KOCH K., BREDE M., BARCZEWSKI M., WALHEIM S., WEIS A., KALTENMAIER A., LEDER A. & BOHN H.F. 2010. The *Salvinia* paradox: superhydrophobic surfaces with hydrophilic pins for air retention under water. Adv. Mater., 22(21): 2325–2328.

BOYD A. 2000. Bennettitales from the Early Cretaceous floras of West Greenland: *Pterophyllum* and *Nilssoniopteris*. Palaeontographica, B, 255: 47–77.

CHEN F., MENG X.Y. & REN S.Q. 1988. The Early Cretaceous flora and coalbearing strata of Fuxin Basin and Tiefa Basin, Liaoning Province. Geological Publishing, Beijing.

CLEAL C.J. & REES P.M. 2003. The Middle Jurassic flora from Stonesfield, Oxfordshire, UK. Palaeontology, 46: 739–801.

CLEAL C.J., REES P.M., ZIJLSTRA G. & CANTRILL D.J. 2006. A clarification of the type of *Nilssoniopteris* Nathorst (fossil Gymnospermophyta, Bennettitales). Taxon, 55(1): 219–222.

CRANE P.R. & HERENDEEN P.S. 2009. Bennettitales from the Grisethorpe Bed (Middle Jurassic) at Cayton Bay, Yorkshire, UK. Am. J. Bot., 96(1): 284–295.

CUTLER D.F., BOTHA T. & STEVENSON D.W. 2007. Plant anatomy: an applied approach. Blackwell Publishing, Malden, USA.

DALIN P., ÅGREN J., BJÖRKMAN C., HUTTUNEN P. & KÄRKKÄINEN K. 2008. Leaf trichome formation and plant resistance to herbivory: 89–105. In: Schaller A. (ed.), Induced plant resistance to herbivory. Springer, Dordrecht.

DENG S.H. 1995. Early Cretaceous flora of Huolinhe Basin, Inner Mongolia, China. Geological Publishing, Beijing.

DENG S.H., REN S.Q. & CHEN F. 1997. Early Cretaceous flora of Hailar, Inner Mongolia, China. Geological Publishing, Beijing.

DENG S.H., ZHAO Y., LU Y.Z., SHANG P., FAN R., LI X., DONG S.X. & LIU L. 2017. Plant fossils from the Lower Jurassic coal-bearing formation of central Inner Mongolia of China and their implications for palaeoclimate. Palaeoworld, 26(2): 279–316.

DUNKIĆ V., BEZIĆ N. & MILETA T. 2001. Xeromorphism of trichomes in Lamiaceae species. Acta Bot. Croat., 60(2): 277–283.

ERDENETSOGT B.O., LEE I., BAT-ERDENE D. & JARGAL L. 2009. Mongolian coal-bearing basins: geological settings, coal characteristics, distribution, and resources. Int. J. Coal Geol., 80(12): 87–104.

EVERT R.F. 2006. Esau's plant anatomy: meristems, cells, and tissues of the plant body: their structure, function, and development. John Wiley & Sons, New Jersey.

FAHN A. 1986. Structural and functional properties of trichomes of xeromorphic leaves. Ann. Bot., 57(5): 631–637.

FAHN A. & CUTLER D.F. 1992. Xérophytes. Gebr, Borntraeger, Stuttgart, Germany.

FLORIN R. 1933. Die Spaltöffnungsapparate der *Williamsonia*-, *Williamsionella*-, und *Wielandiella*-Blüten (Bennettitales). Ark. Bot., 25(A): 1–20.

GIVNISH T.J. 1978. On the adaptive significance of compound leaves with particular reference to tropical trees: 351–380. Tomlinson P.B. & Zimmermann M.H. (eds), Tropical Trees as Living Systems. Cambridge University Press, Cambridge.

GORDENKO N.V. & BROUSHKIN A.V. 2010. A new bennettitalean genus from the Middle Jurassic of the Mikhailovskii Rudnik locality (Kursk Region, Russia). Paleontol. J., 44(10): 1308–1320.

GRAHAM S.A., HENDRIX M.S., JOHNSON C.L., BADAMGARAV D., BADARCH G., AMORY J., PORTER M., BARSBOLD R., WEBB L.E. & HACKER B.R. 2001. Sedimentary record and tectonic implications of Mesozoic rifting in southeast Mongolia. Geol. Soc. Am. Bull., 113(12): 1560–1579.

HARPER J.L., LOVELL P.H. & MOORE K.G. 1970. The shapes and sizes of seeds. Annu. Rev. Ecol. Evol. Syst., 1: 327–356.

HARRIS T.M. 1926. The Rhaetic flora of Scoresby Sound, east Greenland. Medd. Gronl., 68: 44–148.

HARRIS T.M. 1969. The Yorkshire Jurassic flora, III. Bennettitales. Trustees of the British Museum (Natural History), London.

HARRIS T.M. 1973. The Strange Bennettitales. Nineteenth Sir Albert Charles Seward Memorial Lecture. Birbal Sahni Institute of Palaeobotany, Lucknow.

HASEGAWA H., ANDO H., HASEBE N., ICHINNOROV N., OHTA T., HASEGAWA T., YAMAMOTO M., LI G., ERDENETSOGT B.O., HEIMHOFER U. & MURATA T. 2018. Depositional ages and characteristics of Middle–Upper Jurassic and Lower Cretaceous lacustrine deposits in southeastern Mongolia. Island Arc, e12243, https://doi.org/10.1111/iar.12243.

HERRERA F., SHI G., LESLIE A.B., KNOPF P., ICHINNOROV N., TAKAHASHI M., CRANE P.R. & HERENDEEN P.S. 2015. A new voltzian seed cone from the Early Cretaceous of Mongolia and its implications for the evolution of ancient conifers. Int. J. Plant. Sci., 176(8): 791–809.

HERRERA F., LESLIE A.B., SHI G., KNOPF P., ICHINNOROV N., TAKAHASHI M., CRANE P.R. & HERENDEEN P.S. 2016. New fossil Pinaceae from the Early Cretaceous of Mongolia. Botany, 94(9): 885–915.

HERRERA F., SHI G., KNOPF P., LESLIE A.B., ICHINNOROV N., TAKAHASHI M., CRANE P.R. & HERENDEEN P.S. 2017a. Cupressaceae conifers from the Early Cretaceous of Mongolia. Int. J. Plant. Sci., 178(1): 19–41.

HERRERA F., SHI G., ICHINNOROV N., TAKAHASHI M., BUGDAEVA E.V., HERENDEEN P.S. & CRANE P.R. 2017b. The presumed ginkgophyte *Umaltolepis* has seed-bearing structures resembling those of Peltaspermales and Umkomasiales. Proc. Natl. Acad. Sci. U.S.A., 114(12): E2385–E2391.

HERRERA F., MORAN R.C., SHI G., ICHINNOROV N., TAKAHASHI M., CRANE P.R. & HERENDEEN P.S. 2017c. An exquisitely preserved filmy fern (Hymenophyllaceae) from the Early Cretaceous of Mongolia. Am. J. Bot., 104(9): 1370–1381.

ICHINNOROV N. 1996. Lower Cretaceous spores and pollen from the coal deposit Shivee-Ovoo. (summary: Problems of Geology and Mineral Resources in Mongolia, Ulaambaatar).

ICHINNOROV N. 2003. Palynocomplex of the Lower Cretaceous sediments of Eastern Mongolia. Mong. Geosci., 22: 12–16.

ICHINNOROV N., JARGAL L., ODGEREL N. & ENKHTUYA A. 2012. Palynology and petrology characteristics of the Lower Cretaceous Tevshiin Gobi coal deposit, Mongolia. 11th Symposium on Mesozoic Terrestrial Ecosystems. August 15–18, Korea.

JOHNSON H.B. 1975. Plant pubescence: an ecological perspective. Bot. Rev., 41(3): 233–258.

KVAČEK J. 1995. Cycadales and Bennettitales leaf compressions of the Bohemian Cenomanian, Central Europe. Rev. Palaeobot. Palynol., 84: 389–412.

KRASSILOV V.A. l967. Early Cretaceous floras from South Primorye and its significance of stratigraphy. Nauka, Moscow (in Russian).

KRASSILOV V.A. 1973. Materials on the stratigraphy and taphofloras of the coal-bearing strata of Bureja Basin: 28–51. In: V.A. Krassilov (ed.), Fossil Floras and Phytostratigraphy of the Far East. Akademia NAUK SSSR, Vladivostock.

KRASSILOV V.A. 1981. Changes of Mesozoic vegetation and the extinction of dinosaurs. Palaeogeogr. Palaeoclimatol. Palaeoecol., 34: 207–224.

KRASSILOV V.A. 1982. Early Cretaceous flora of Mongolia. Palaeontographica, B, 181: 1–43.

KERP H. & KRINGS M. 1999. Light microscopy of cuticles: 52–56. In: Jones T.P. & Rowe N.P. (eds), Fossil plants and spores: modern techniques. Geological Society, London

LESLIE A.B., GLASSPOOL I., HERENDEEN P.S., ICHINNOROV N., KNOPF P., TAKAHASHI M. & CRANE P.R. 2013. Pinaceae-like reproductive morphology in *Schizolepidopsis canicularis* sp. nov. from the Early Cretaceous (Aptian-Albian) of Mongolia. Am. J. Bot., 100(12): 2426–2436.

LEVIN D.A. 1973. The role of trichomes in plant defense. Q. Rev. Biol., 48(1): 3–15.

LI X.X., YE M.N. & ZHOU Z.Y. 1986. Late Early Cretaceous flora from Shansong, Jiaohe, Jilin, northeastern China. Palaeontol. Cathayana, 3: 1–143.

MANUM S.B., BOSE M.N. & VIGRAN J.O. 1991. The Jurassic flora of Andøya, northern Norway. Rev. Palaeobot. Palynol., 68(3–4): 233–256.

MARKEVICH V.S. & BUGDAEVA E.V. 2014. Late Jurassic-Early Cretaceous coal-forming plants of the Bureya Basin, Russian Far East. Stratigr. Geol. Correl., 22(3): 239–255.

NA Y., SUN C., DILCHER D.L., WANG H., LI T. & LI Y. 2014. *Nilssoniopteris binggouensis* sp. nov. (Bennettitales) from the Lower Cretaceous of northeast China. Int. J. Plant. Sci., 175(3): 369–381.

NATHORST A.G. 1909. Über die Gattung *Nilssonia* Brongn. mit besonderer Berü cksichtigung schwedischer Arten. K. Sven. Vetensk. Akad. Handl., 43: 1–40.

NICHOLS D.J., MATSUKAWA M. & ITO M. 2006. Palynology and age of some Cretaceous nonmarine deposits in Mongolia and China. Cretac. Res., 27: 241–251.

PENNY J.H. 1999. Extraction of lignitic and fusainized plant fragments from unconsolidated sandy and clay-rich sediments: 9–10. In: Jones T.P. & Rowe N.P. (eds), Fossil plants and spores: modern techniques. Geological Society, London.

POTT C. & MCLOUGHLIN S. 2014. Divaricate growth habit in Williamsoniaceae (Bennettitales): unravelling the ecology of a key Mesozoic plant group. Palaeobio. Palaeoenv., 94: 307–352.

POTT C. & VAN KONIJNENBURG-VAN CITTERT J.H. 2017. The type specimen of *Nilssoniopteris solitaria* (Phillips 1829) Cleal et P.M. Rees 2003 (Bennettitales). Acta Palaeobot., 57(2): 177–184.

POTT C., KRINGS M. & KERP H. 2007. First record of *Nilssoniopteris* (Gymnospermophyta, Bennettitales) from the Carnian (Upper Triassic) of Lunz, Lower Austria. Palaeontology, 50(5): 1299–1318.

POTT C., KRINGS M., KERP H. & FRIIS E.M. 2010. Reconstruction of a bennettitalean flower from the Carnian (Upper Triassic) of Lunz, Lower Austria. Rev. Palaeobot. Palynol., 159: 94–111.

POTT C., MCLOUGHLIN S., WU S. & FRIIS E.M. 2012. Trichomes on the leaves of *Anomozamites villosus* sp. nov. (Bennettitales) from the Daohugou beds (Middle Jurassic), Inner Mongolia, China: Mechanical defence against herbivorous arthropods. Rev. Palaeobot. Palynol., 169: 48–60.

POTT C., SCHMEIßNER S., DÜTSCH, G. & VAN KONIJNENBURG-VAN CITTERT J.H. 2016. Bennettitales in the Rhaetian flora of Wüstenwelsberg, Bavaria, Germany. Rev. Palaeobot. Palynol., 232: 98–118.

RAY M.M., ROTHWELL G.W. & STOCKEY R.A. 2014. Anatomically preserved Early Cretaceous bennettitalean leaves: *Nilssoniopteris corrugata* n. sp. from Vancouver Island, Canada. J. Paleontol., 88(5): 1085–1093.

SCHWEITZER H.J. & KIRCHNER M. 2003. Die rhätojurassischen Floren des Iran und Afghanistans. 13. Cycadophyta III. Bennettitales. Palaeontographica, B, 264: 1–166.

SHI G., LESLIE A.B., HERENDEEN P.S., ICHINNOROV N., TAKAHASHI M., KNOPF P. & CRANE P.R. 2014. Whole-plant reconstruction and phylogenetic relationship of *Elatides zhoui* sp. nov. (Cupressaceae) from the Early Cretaceous of Mongolia. Int. J. Plant Sci., 175(8): 911–930.

SHI G., LESLIE A.B., HERENDEEN P.S., HERRERA F., ICHINNOROV N., TAKAHASHI M., KNOPF P. & CRANE P.R. 2016. Early Cretaceous *Umkomasia* from Mongolia: implications for homology of corystosperm cupules. New Phytol., 210(4): 1418–1429.

SHI G., HERRERA F., HERENDEEN P.S., LESLIE A.B., ICHINNOROV N., TAKAHASHI M. & CRANE P.R. 2018. Leaves of *Podozamites* and *Pseudotorellia* from the Early Cretaceous of Mongolia: stomatal patterns and implications for relationships. J. Syst. Palaeontol., 16(2): 111–137.

SHI G., CRANE P.R., HERENDEEN P.S., ICHINNOROV N., TAKAHASHI M., & HERRERA F. (in press). Diversity and homologies of corystosperm

seed-bearing structures from the Early Cretaceous of Mongolia. J. Syst. Palaeontol., DOI 10.1080/14772019.2018.1493547

SINCOCK C.A. & WATSON J. 1988. Terminology used in the description of bennettitalean cuticle characters. Bot. J. Linn. Soc., 97(2): 179–187.

SOH W.K., WRIGHT I.J., BACON K.L., LENZ T.I., STEINTHORSDOTTIR M., PARNELL A.C. & MCELWAIN J.C. 2017. Palaeo leaf economics reveal a shift in ecosystem function associated with the end-Triassic mass extinction event. Nat. Plants, 3: 17104. DOI:10.1038/nplants.2017.104.

STEINTHORSDOTTIR M., WOODWARD F.I., SURLYK F. & MCELWAIN J.C. 2012. Deep-time evidence of a link between elevated $CO_2$ concentrations and perturbations in the hydrological cycle via drop in plant transpiration. Geology, 40(9): 815–818.

SUN B.N. & SHEN G.L. 1988. A new species of genus *Nilssoniopteris*. Acta Palaeontol. Sin., 5: 561–564.

SUN B.N. & YANG S. 1988. A supplementary study of fossil plants from the Xiangxi Formation, western Hubei. J. Lanzhou. Univ. S1: 84–91.

THOMAS H.H. 1916. On *Williamsoniella*, a new type of bennettitalean flower. Philos. Trans. R. Soc. Lond. B Biol. Sci., 207: 113–148.

THOMAS B.A. & BATTEN D.J. 2001. The Jurassic palaeobotany of Yorkshire: 29–96. In: Cleal, C.J., Thomas B.A., Batten D.J., & Collinson M.E. (eds), Mesozoic and Tertiary palaeobotany of Great Britain. Joint Nature Conservation Committee, Peterborough, UK.

TOZIN L.R.S., SILVA DE MELO S.C. & RODRIGUES T.M. 2016. Non-glandular trichomes in Lamiaceae and Verbenaceae species: morphological and histochemical features indicate more than physical protection. N.Z.J. Bot., 54(4): 446–457.

TRYON A.F. 1965. Trichomes and paraphyses in ferns. Taxon, 14(7): 214–218.

VAN KONIJNENBURG-VAN CITTERT J.H., POTT C., CLEAL C.J. & ZIJLSTRA G. 2017. Differentiation of the fossil leaves assigned to *Taeniopteris*, *Nilssoniopteris* and *Nilssonia* with a comparison to similar genera. Rev. Palaeobot. Palynol., 237: 100–106.

WANG Z.Q. 1984. Plant kingdom: 223–302. In: Palaeontological Atlas of North China: Mesozoic volume. Geological Publishing, Beijing (in Chinese).

WAR A.R., PAULRAJ M.G., AHMAD T., BUHROO A.A., HUSSAIN B., IGNACIMUTHU S. & SHARMA H.C. 2012. Mechanisms of plant defense against insect herbivores. Plant Signal Behav., 7(10): 1306–1320.

WATSON J. & SINCOCK C.A. 1992. Bennettitales of the English Wealden. Monogr. Palaeontogr. Soc., 145: 2–228.

WATSON J. & ALVIN K.L. 1996. An English Wealden floral list, with comments on the possible environmental indicators. Cretac. Res., 17(1): 5–26.

WEI W., SUN Y. & WANG Y. 2005. *Nilssoniopteris* from the Lower Cretaceous Changcai Formation in Yanbian area of Jilin, China. Global Geology, 24: 1–6.

WELLMAN C. & AXE L.1999. Extracting plant mesofossils and megafossils by bulk acid maceration: 11–14. In: Jones T.P. & Rowe N.P. (eds), Fossil plants and spores: modern techniques. Geological Society, London.

WERKER E. 2000. Trichome diversity and development. Adv. Bot. Res., 31: 1–35.

WHITE P.S. 1983. Corner's rules in eastern deciduous trees: allometry and its implications for the adaptive architecture of trees. Bull. Torrey Bot. Club., 110: 203–212.

WOOD A.J. 2005. Eco-physiological adaptations to limited water environments: 1–13. In: Jenks M.A. & Hasegawa P.M (eds), Plant Abiotic Stress. Blackwell Publishing, Oxford.

WU X.W. 1988. Some plants of Bennettitales from middle Jurassic Hsiangchi Formation in west Hubei, China. Acta Palaeontol. Sin., 27: 751–758.

WU X.W. 1993. Record of generic names of Mesozoic megafossil plants from China (1865–1990). Nanjing University Press, Nanjing.

YAMADA T., LEGRAND J. & NISHIDA H. 2009. Structurally preserved *Nilssoniopteris* from the Arida Formation (Barremian, Lower Cretaceous) of southwest Japan. Rev. Palaeobot. Palynol., 156: 410–417.

ZHANG W., ZHANG Z.C. & ZHENG S.L. 1980. Plant kingdom: 221–339. In: Palaeontological atlas of northeast China: Mesozoic and Cenozoic volume. Geological Publishing, Beijing (in Chinese).

ZHAO Y., DENG S., SHANG P., LENG Q., LU Y., FU G. & MA X. 2018. Two new species of *Nilssoniopteris* (Bennettitales) from the Middle Jurassic of Sandaoling, Turpan-Hami Basin, Xinjiang, NW China. J. Paleontol., 1–21. https://doi.org/10.1017/jpa.2017.133.

ZHENG S.L. & ZHANG W. 1982. Fossil plants from Longzhaogou and Jixi Groups in eastern Heilongjiang Province. Shenyang Inst. Geol. Mine Resour., 7: 68–98 (in Chinese).

ZHENG S.L., ZHANG W. & ZHANG Y. 1990. A new species of genus *Nilssoniopteris* from the Early Cretaceous of Hailar Basin. J. Integr. Plant Biol. 32: 483–489.

ZHOU Z.Y. 1989. Late Triassic plants from Shaqiao, Hengyang, Hunan Province. Palaeontol. Cathayana, 4: 131–159.